SIMULATION OF FREE SPACE OPTICAL LINKS UNDER DIFFERENT
ATMOSPHERIC CONDITIONS

A THESIS SUBMITTED TO
THE GRADUATE SCHOOL OF NATURAL AND APPLIED SCIENCES
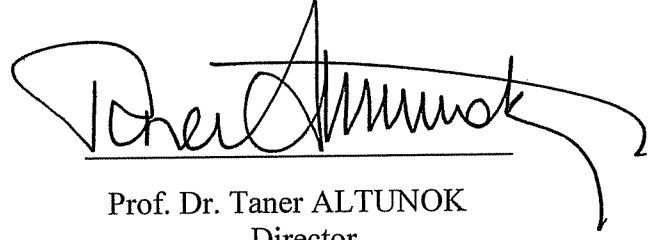OF
ÇANKAYA UNIVERSITY

BY

KORHAN ÖZTÜRK

IN PARTIAL FULFILLMENT OF THE REQUIREMENTS
FOR
THE DEGREE OF MASTER OF SCIENCE
IN
ELECTRONICS AND COMMUNICATION ENGINEERING

DECEMBER 2011

Title of the Thesis :   **SIMULATION OF FREE SPACE OPTICAL LINKS UNDER DIFFERENT ATMOSPHERIC CONDITIONS**

Submitted by **Korhan ÖZTÜRK**

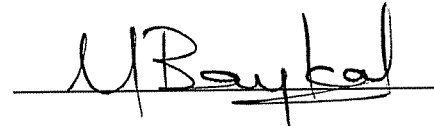Approval of the Graduate School of Natural and Applied Sciences, Çankaya University

Prof. Dr. Taner ALTUNOK
Director

I certify that this thesis satisfies all the requirements as a thesis for the degree of Master of Science.

Prof. Dr. Celal Zaim ÇİL
Head of Department

This is to certify that we have read this thesis and that in our opinion it is fully adequate, in scope and quality, as a thesis for the degree of Master of Science.

Prof. Dr. Yahya Kemal BAYKAL
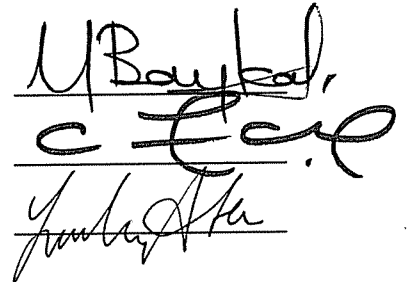Supervisor

Examination Date: 24.08.2011

Examining Committee Members

Prof. Dr. Yahya Kemal Baykal   (Çankaya Univ.)

Prof. Dr. Celal Zaim ÇİL   (Çankaya Univ.)

Dr. Yalçın ATA   (TUBİTAK-SAGE)

STATEMENT OF NON-PLAGIARISM

I hereby declare that all information in this document has been obtained and presented in accordance with academic rules and ethical conduct. I also declare that, as required by these rules and conduct, I have fully cited and referenced all material and results that are not original to this work.

Name, Last Name : Korhan ÖZTÜRK

Signature :

Date : 09. 12 . 2011

ABSTRACT

SIMULATION OF FREE SPACE OPTICS LINKS UNDER DIFFERENT
ATMOSPHERIC CONDITIONS

ÖZTÜRK, Korhan

M.Sc., Department of Electronics and Communication Engineering

Supervisor: Prof. Dr. Yahya Kemal BAYKAL

December 2011, 57 pages

This thesis contains a feasibility study for the free space optical links, which would be installed in Turkey. In first chapters, some basic information and the background theory of the atmospheric channel are given. Predefined optical links are simulated with PCModWin-MODTRAN radiative transfer code to investigate the link availability under the influence of different weather conditions. In addition, numerical calculations according to some experimentally approved models are also performed and these results are compared with the results of simulations. For all these simulations and calculations, big amount of meteorological data was collected from the airport stations, which are in different cities in Turkey. The parameters used in calculations were supplied from the commercially available FSO systems.

In conclusion, the effectiveness of FSO links in Turkey is discussed.

Keywords: Free Space Optics, PCModWin, Link Availability, Optical Wireless Communication.

ÖZ

SERBEST UZAY HABERLEŞME LİNKLERİNİN DEĞİŞİK METEOROLOJİK KOŞULLAR ALTINDA SİMULASYONU

ÖZTÜRK, Korhan

Yükseklisans, Elektronik ve Haberleşme Mühendisliği Anabilim Dalı

Tez Yöneticisi: Prof. Dr. Yahya Kemal BAYKAL

Aralık 2011, 57 sayfa

Bu tez, Türkiye'de kurulması planlanan FSO linkleri için bir fizibilite çalışmasını içermektedir.Bazı temel bilgiler ve atmosferik kanal teorisi anlatıldıktan sonra, değişik hava şartları altındaki link erişilebilirliğini araştırmak amacıyla daha önceden tanımlanan linkler PCModWin programı aracılığıyla simule edilmiştir. Ayrıca, bahsedilen empirik modeller ile PCModWin sonuçları karşılaştırılmıştır. Tüm bu simulasyon ve hesaplamalar için, Türkiye'nin çeşitli bölgelerindeki havaalanlarından alınan meteorolojik veriler ile piyasada ticari olarak bulunabilen cihazlara ait parametreler kullanılmıştır.

Sonuç olarak, Türkiye'de FSO bağlantılarının etkinliği tartışılmıştır.

Anahtar Kelimeler: Serbest Uzay Haberleşmesi,PCModWin, Hat Erişilebilirliği, Kablosuz Optik Haberleşme.

ACKNOWLEDGMENTS

TABLE OF CONTENTS

LIST OF TABLES

TABLES

LIST OF FIGURES

FIGURES

CHAPTER 1

INTRODUCTION

Recent developments in semiconductor technology and the detailed researches about the atmospheric attenuation and turbulence have made free space optical (FSO) communication links a viable option to microwave links and fiber cables for short-haul broadband links [1,2]. In comparison with the microwave technology, an FSO link provides more bandwidth without interference and interception. In addition, because of the operating wavelength, there is no need for licensing. Advantages over fiber are the quick installation time and cheap equipment with a high portability [3].

On the other hand, beside the advantages of an FSO system over fiber and microwave links, there are still challenges for FSO that affect the overall availability of the link. Due to weather dependent challenges, which are very variable, it is difficult to predict the total attenuation and the other effects. Therefore, in severe attenuation conditions, the operation of an FSO link cannot be maintained at all time and the availability reduces. In order to achieve a high available link, a various methods are suggested like radio frequency (RF)/FSO hybrid links [2], various network topologies [4], wavelength-division multiplexing (WDM) links [5,6], different modulation types [7,8] and the different wavelength selections [9,10].

To estimate the link availability performance from link parameters, some standard models which use atmospheric visibility are derived [11,12,13]. Also the attenuations

caused by precipitation [1] and scintillation [14,15,16] are defined. Thus, the availability can be estimated considering the total attenuation, which is calculated with these models, and the total amount of attenuation can be tolerated by a given system at a given range. The availability can be defined as the ratio of total time that atmospheric attenuation is lower than the total amount of attenuation that can be tolerated by FSO system to total transmission time.

To investigate the impact of atmospheric effects on the link availability, a multiple FSO field-trial had been deployed during 2001 in the surrounding area of Milan [17]. In this trial, estimated attenuations with collected data were corrected with measured attenuations. On the other hand, instead of self-measurement, using the historical data that retrieved from the meteorological stations of airports is another way to estimate the attenuation. In another study, which was based on long-term meteorological visibility observations, some realistic results for estimating FSO performance in Europe was shown in [18]. With the same idea, a first attempt at an FSO availability map for U.S.A was also presented in [19]. In addition, similar studies were performed for a test link in Ankara and some valuable results were obtained [2,20].

1.1. OBJECTIVE OF THE THESIS

In this thesis, link availability analyses for different cities along the year 2010 are performed to estimate the FSO performance in Turkey. The link availability calculation in this work is based on same power budget analysis with the studies mentioned above [2,18-20]. However, power losses due to scattering, absorption and precipitation are modeled by PCModWin (MODTRAN) code using visibility and precipitation data collected during 2010 year at three airports in Turkey. By using PCModWin, we aimed to get more accurate results rather than using empirical models. In addition, power loss caused by scintillation and geometry of the link is modeled using ITU-R Report F.2106.

1.2.   THESIS STRUCTURE

This thesis was organized as follows:

The first chapter is the Introduction, mainly providing the background and a literature review on related topics. This chapter also includes the objective of the study.

The second chapter concentrates on the FSO technology and its advantages, disadvantages and the applications.

In the third chapter, the atmospheric channel model is given and theoretical background of the analyses that will be mentioned in chapter five is completed.

The fourth chapter discussed the availability concept, which was used in our study. Meteorological data, manufacturer parameters and some information about the PCModWin software were given.

Results of the analyses are given in the fifth chapter. Link availability graphs for different cities and different months are investigated. With comparative graphs the geographical, seasonal and equipment dependent differences between pre-defined cases are shown.

In the sixth chapter, comments about the results of the analyses and some suggestions to increase the link availability and performance are given.

CHAPTER 2

FREE SPACE OPTICAL COMMUNICATION TECHNOLOGY

2.1.   OVERVIEW

The increasing number of high bandwidth demanding services all over the world leads developers to find new communication techniques for the end user. Popular fiber-to-the-home (FTTH) services deliver these high data rates to the consumer but fiber is generally not available or the cabling costs are too high. At that point, free space optics (FSO) excels with high data rates and low costs as an end user solution.

FSO, also known as optical wireless communication (OWC), uses infrared waves as carrier signal and the atmosphere, water or vacuum as transmission medium. Because of the availability of low cost laser diodes, the commercial FSO systems are operated near the infrared region of the electromagnetic spectrum (at wavelengths between 750 nm to 850 nm). Positive intrinsic negative (PIN) and avalanche photodiode (APD) receivers are also available and FSO systems can be operated at 2,7 Gb/s rate at these wavelengths. However, the demand of more bandwidth for longer ranges has pushed the operation of these systems to longer wavelengths where laser diodes can provide more optical power (between 1500nm-1650nm). In addition, Erbium-doped fiber amplifiers (EDFAs), which allows for more optical power can be used at these wavelengths and thus the range of the system can be increased.

Today, there are many varieties of FSO applications on the market. Short-range wireless communication links providing network access to mobile devices, last-mile links between end users and existing fiber optic communication backbones, secured military applications and laser communications in outer-space links are some examples for these existing applications. Among them, indoor wireless applications also have become very popular in recent years. Generally, indoor optical wireless communication is known as wireless infrared communication and outdoor optical wireless communication is commonly known as free space optical (FSO) communication. In this study, we concerned with outdoor and terrestrial optical wireless communication applications.

FSO technology provides broadband communication capacity using unlicensed optical wavelengths. If we compare the technologies, faster installation, lower cost and no need for permission to lay cables into the ground make FSO preferable to fiber technology. High data rates, secured communication channel with narrow beam angle, unlicensed wavelengths and easy operation make preferable FSO to microwave technology.

However, when communicating through atmospheric channel, the received signal is open to undepicted attenuation because of the weather conditions. In addition, inhomogeneity in the temperature and pressure of the atmosphere cause refractive index variations. These refractive index variations cause optical intensity fluctuations on receiver which results as fading. These faded links cause performance degradation because of increased bit error rate (BER) and transmission delays.

2.2. ADVANTAGES OF FSO

The biggest advantage of FSO links is low cost. In most cases, the cost of digging the streets to lay cables and the difficulties of obtaining right-of-way permits make FSO an attractive alternative. For example, in urban areas one mile (1,6km) fiber deployment could cost $100,000-$200,000 and a fixed RF wireless solution could cost $30,000. By contrast, a short 155 Mbps FSO link might cost only $ 18,000 [21].

Another advantage of FSO technology is the high bandwidth availability, which could provide broadband wireless connections from fiber backbones to end-users. Today, radio frequency (RF) technology can support much longer links than FSO technology, but its bandwidth is up to 622 Mbps. On the other hand, available FSO systems support 2,7 Gbps and these capacities are growing. For example, a 160 Gbps-FSO-link has been successfully tested in laboratories with WDM technology [46]. These rates will be able to reach the Tbps range in a short period.

When we compared to fiber communication, there are really cost and time saving advantages of FSO. For example, FSO installation does not require digging streets and there is no need for permission from authorities for installation. In addition, FSO equipment is generally placed on a roof or even behind a window only in a few hours. Also, the equipment can be redeployed to another location easily. FSO terminals are portable and quickly deployable. With all this advantages, FSO is very suitable for disaster recovery and temporary installations like concerts or festivals.

Another advantage is that there is no need for licensing or frequency allocating for FSO links because frequencies greater than 300 GHz are unregulated. Frequency allocation for microwave transmission is generally very difficult and costly in some urban areas or near airports. In addition, customer base is not limited to frequency license holders.

Detection, interception and jamming are common security problems for classical microwave links. However, the narrow beam of the laser makes FSO links very resistant against these kinds of security problems. To not block the FSO link, equipment is generally installed as far as possible from moving things. For example, beam tapping requires a mirror or another device which remains in the beam path for extended periods. But users of the system can immediately notice that the beam is interrupted. Because of its superior security to RF-transmission, FSO is suitable for financial, legal, military or other sensitive information transmission [22].

2.3. DISADVANTAGES OF FSO

One of the biggest problems is the effect of weather conditions on signal transmission. This limitation causes the range problem on FSO links. For instance, commercially available FSO systems generally have a maximal range of only 500 m when thick fog reduces the visibility to only 200 m. Fog represents the greatest challenge, because the water particles are small and dense enough to diffract the light pulse and extinct the signal. The particles of rain and snowfall are larger than the used wavelength, thus they affect the transmission less than fog [23].

Because of the FSO requires a free line of sight, a pre-installation site evaluation must be done to ensure that the paths between the FSO units are clear and will remain for a long time. The growth of trees and the construction of buildings need to be considered. Also, birds can block the beam temporarily. If a bird (or any other object) crosses the beam the data transmission will be interrupted for a short duration. Ethernet and Token Ring can handle such interrupts and will retransmit the data as per protocol.

Environmental conditions such as wind can cause building movements and these effects can disrupt the receiver and transmitter alignment. To mitigate these effects, FSO systems use two approaches. First, a broader beam divergence angle can be used. Second, active tracking systems can be used to keep beam aligned. Latest technology FSO systems use multiple lasers, motorized gimbal mounts and quad detectors to overcome building movement problems.

Another problem for FSO communication links is scintillation. Heated air rising from the ground or rooftops creates temperature variations among different air pockets. As a result, the refractive index varies in time along the link which causes scintillations over the beam. These scintillations appear as power fluctuation in the receiver.

2.4. APPLICATIONS

Until recent years, FSO technology was used for enterprise connectivity, for example mainly in local-area networks between multiple buildings, where right of way is an obstacle to lay fiber-optic cable. But in the recent years, FSO have started to move into more backbone connections. Several FSO companies have started field trials with biggest carriers of the United States, Europe, Asia, South America and the Middle East. Although, an estimated 95 percent of buildings are within 1.5 km of fiber optic infrastructure in the United States, they are unable to access it. Connecting them with fiber can cost US $100,000-$200,000/km in metropolitan areas, with 85 percent of the total cost caused by trenching and installation [24]. Instead of spending this money, installing FSO links gives a big opportunity to reduce the costs for carriers.

Carriers can extend their existing metropolitan area fiber rings by connecting new networks to their core network with FSO. Also, SDH/SONET rings can be completed or back up by FSO links.

On the other hand, FSO can also be a good solution for the broadband wireless access technology that can support the high bandwidth requirements of a last-mile wireless broadband access. FSO can be used to connect end users with Internet service providers or other networks.

The rapid deployment, portability, high bit rate and especially the security make FSO a very interesting alternative for military applications.

Because of its omnidirectional structure and the experienced technology, most tactical communication systems use the RF spectrum. Radio offers enough bandwidth for voice communications, but it is not enough for situational awareness displays and high resolution images. The tactical weakness of RF provides an opportunity to detect, intercept, exploit or target using direction finding or homing systems. In addition, modern scanners have both wide frequency band coverage and rapid scan rates, thus detection of radio transmissions is quite easy.

Out of the terrestrial links, the optical link techniques are also applied the inter orbit satellite communication systems. Actually, due to no absorption of optical signals by the air in the outer space, the optical link in the outer space has a potential to transmit much longer distance than the terrestrial links.

At the beginning of the year 2000, the first laser transmission and high communication rate between two satellites had taken place. In November 2001, there was a successful link between the French satellite Spot-4 and the European satellite Artemis separated from each other by thousands of kilometers [25].

The latest projects concerning Earth to satellite communications are directed towards a 2000-kilometer distance laser communication at 1 Gbps and higher rates.

Another common optical communication application is the indoor optical wireless system which is known as Infrared Communication. In indoor communication, laser diodes (LDs) or light emitting diodes (LEDs) are used as transmitter and photodiodes as the receivers. These optoelectronic devices are cheaper as compared to RF equipment as well as wire line systems. Furthermore, optical transmission does not interfere with existing RF systems. The infrared signal does not penetrate walls, thus providing privacy within the office area. In addition, building a cell-based network is easier with this feature. For example, in an office building each room would be a cell and there would be no interference between the cells. So, all units can be identical in a cellular architecture. However, in RF configuration operating frequencies of neighboring cells have to be different. Due to the above reasons, optical wireless systems are becoming more popular in various operating environments, such as houses, offices, medical facilities, manufacturing plants, and business establishments [26].

2.5.   STANDARDIZATION

IrDA (Infrared Data Association)

IrDA is an example of indoor free space optical communication with very short-range and it is generally used in medical instrumentation, test and measurement equipment, mobile phones and computers. The Infrared Data Association (IrDA) defines physical specifications communications protocol standards for the short-range exchange of data over infrared light [27].

ITU-R (International Telecommunication Union – Radio Section)

Performance and characteristics of free-space optical communication systems are discussed within ITU-R WP5C (Working Party 5C). One report (ITU-R F.2106) on the fixed service applications using free-space optical links was submitted to WP5C and approved as ITU-R Report. In this report, characteristics, applications and other technical aspects of free space optical links are summarized for the fixed services. This report also includes ITU-R P.1814 and ITU-R P.1817 recommendations. The optical attenuation characteristics in the fog, rain and snow are clearly described in these reports [28].

2.6.   EYE SAFETY

Eye safety is also an important subject. High power laser beam can cause serious injuries to the eye and even to the skin. High laser power within the wavelengths between 400 nm to 1400 nm is absorbed by the eye into the retina and can cause retina damage. Wavelengths over 1400 nm may also damage the lens and the cornea. Because of these reasons, many countries and organizations have created and defined the laser safety standards, which have to be fulfilled by the manufacturers and the service providers.

In general, the safety standards give guidelines about the safety of the FSO system equipment and the safety of the users. Class 1 lasers and the Class 1M lasers are the two most important classifications. Under reasonably operating conditions, Class 1

10

lasers are considered as safe and the Class 1M lasers should only be installed in locations where the unsafe use of optical aids can be prevented [29].

CHAPTER 3

ATMOSPHERIC CHANNEL MODEL

In FSO communication links, absorption of the beam by the atmosphere is very important, especially in adverse weather conditions of fog, snow or heavy rain. In our study, we investigated the reasons of link attenuation to model the atmospheric channel. First, nature events that lead to attenuation will be mentioned. Later, empirical models will be discussed and comparative graphs between these models and PCModWin(MODTRAN) results will be compared.

3.1. ATMOSPHERIC EFFECTS ON FSO SYSTEMS

3.1.1. RAIN

Rain has a negative impact on FSO because the mean radius of raindrops is larger than the wavelength of FSO light beam. Typical rain attenuation values are generally moderate or weak in nature. For example, a rainfall rate of 2,5 mm/hour can cause 6 dB/km signal attenuation. Therefore, 25 dB link margin of a commercially available FSO system can easily penetrate this rain attenuation. However, when the rain rate increases to 100 mm/hour level, rain attenuation can become a serious issue even for 25dB link margin. But, this kind of rain can be seen only for a short period. An attractive point about RF wireless technologies, which use frequencies above 10 GHz, is they are impacted adversely by rain and little influenced by fog because the

mean radius of raindrops is closer to RF wavelengths. The lower RF frequencies in the 2.4 GHz-5.8 GHz ranges relatively unaffected by rain or fog, but due to they are license free, in those frequencies a new problem which is called as interference raises.

3.1.2. SNOW

Snowflakes are ice crystals which have a variety of shapes and sizes. Snowflakes are generally larger than rain drops, thus the attenuation caused by snow is so much weak compared to fog and heavy rain. On the other hand, whiteout conditions can attenuate the beam, but scattering is not a big problem for FSO systems, because the size of snowflakes is large when compared to the operating wavelength. The impact of light snow to whiteout conditions falls approximately between light rain to moderate fog, with a potential link attenuation varies between 3 dB/km to 30 dB/km.

3.1.3. FOG

Because the small water droplets, which compose the fog, have a radius about the size of FSO wavelengths, fog is the most important weather event for optical communication. The size distribution of the particles varies for different densities of fog. Generally, when visibilities range between 0–2,000 meters, weather condition is referred as fog. Descriptive words like "dense fog" or "thin fog" are sometimes used to characterize the appearance of fog.

Fog characteristic is not comprehensible because characterizing the fog physically is very difficult. Although there are some methods like particle size and density measurements to describe fog conditions in a quantitative way, visibility is most commonly used to characterize foggy conditions. The FSO community also uses visibility data, which have been taken at airports for a long time, as the main parameter for the fog. The airport measurements give some statistical availability figures for FSO systems and allow characterizing different regions. Generally, the temporal resolution of these data is not very high, although most of the data has been

collected over years. For the microclimate environments like sea or rivers side, can induce foggy conditions, thus the airport data sometimes is not reliable enough for all environments. However, airports are typically located outside metropolitan boundaries and the microclimate inside a city typically generates less foggy conditions. Thus, the estimation with those data can be acceptable for the minimum link availability level. Another problem is the density distribution of fog particles can also vary with height and this makes the modeling of fog even more complex. The limited and unreliable information about fog is definitely one of the biggest problems for the FSO world.

3.1.4. TURBULENCE

After the discussion of severe effects of weather, the infinite space like desert might seem the perfect environment for an FSO link. If we only concern about the attenuation of the atmosphere, this could be true. However, in hot and dry climates like deserts, another problem raises with the transmission called as turbulence.

Turbulence is generally defined as the changes of the path of light due to the changes of the refractive index of air pockets. In a sunny day, some air cells or air pockets heat up more than others do. This causes changes in the refractive index along the path of the light while it propagates through the air. The refractive index changes in a random motion because these air pockets are not stable in time and space. This behavior appears as turbulent for the outside observer.

Laser beams experience three effects under turbulence. First, due to the changing refractive index cells, the beam can be deflected randomly through the path. This is generally known as beam wander. Second, the phase front of the beam can vary, producing intensity fluctuations or scintillation. Third, the beam can spread more than diffraction theory predicts [34].

3.2. LINK BUDGET

If we design an FSO link, we should consider the link budget as a key parameter. After calculating all the losses, which can affect the link, available power should be above the sensitivity of the receiver. In this chapter, link budget equation, all kind of attenuations that disrupt the link and the models to predict these attenuations will be mentioned.

The mean optical power P_R on the receiving aperture of an FSO terminal can be given by the link budget equation;

$$P_R = P_T - L_{SYS} - L_{GEO} - L_{ATM} \tag{3.1}$$

where P_T is the mean optical power on transmitting side, L_{SYS} is constant loses due to coupling and other system connections, L_{GEO} is the geometric loss due to structure of the beam and the L_{ATM} is the loses due to atmospheric influences. Now, each attenuation component will be investigated in order.

3.2.1. GEOMETRIC ATTENUATION

Spreading of the transmitted beam between the transmitter and the receiver causes geometric attenuation. Due to the geometric attenuation, even in clear weather conditions, detector receives less signal power. Geometric losses can be approximated by using the following formula [30].

$$L_{GEO} = -10 \, log \left(\frac{D_{RX}}{D_{TX} + \theta L} \right)^2 \tag{3.2}$$

where, D_{RX} and D_{TX} are receiver and transmitter antenna apertures in m, L is the distance between the transmitter and the receiver measured in km and θ is the divergence of the transmitted laser beam in mrad.

This model could approximate the geometric losses for a Gaussian power distribution but with a less accuracy because it assumes a uniform power distribution.

In our study, it was seen that geometrical attenuation forms the largest part of the total link attenuation. Even in moderate fog or heavy rain events, geometrical attenuation could be still a major effect for links, which has a range over 1 kilometer. Fig.1 shows geometrical attenuation and link distance relation of FSO system that was used in this study.
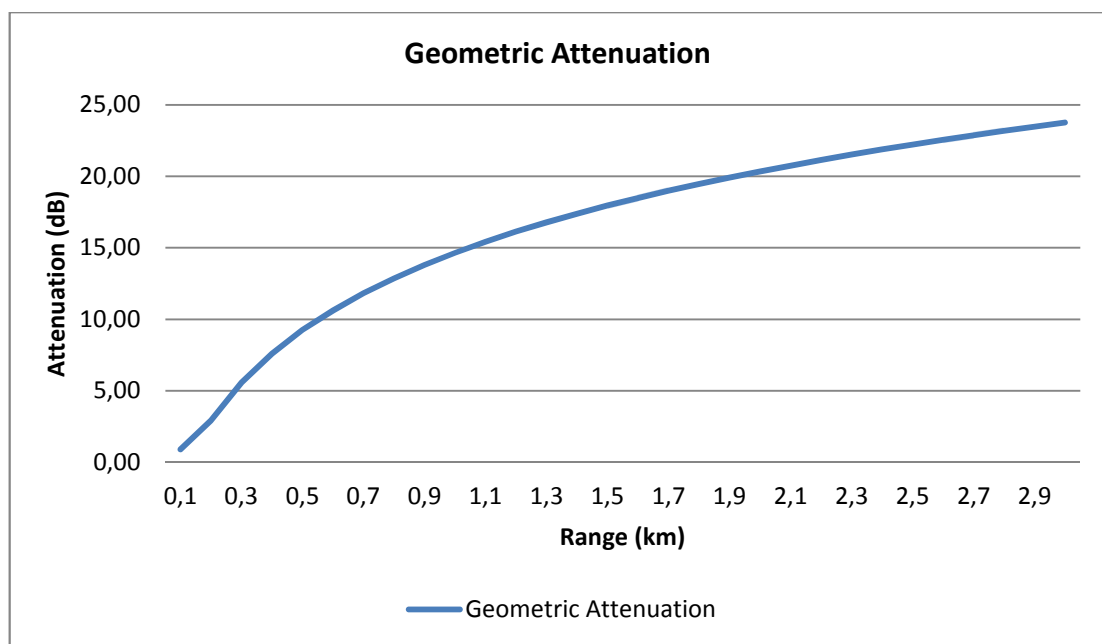
Figure 1 Geometrical Attenuation vs Link Distance Graph.

3.2.2. SYSTEM ATTENUATION

System attenuation represents all the system dependent attenuations. This includes coupling losses, transmitter-receiver losses, misalignment losses and solar radiation

losses. In our study, after some catalogue review, we assumed system attenuation as 6 dB for each link.

3.2.3. ATMOSPHERIC ATTENUATION

Atmosphere interacts with light due to the composition of the atmosphere, which normally consists of different molecular species and small-suspended particles called aerosols. This interaction produces three major effects, which are absorption, scattering and scintillation.

The attenuation due to atmospheric effects can be calculated using various models available in propagation literature. The attenuation of the laser power in the atmosphere is described by Beer's law [31],

$$\tau(R) = \frac{P(R)}{P(S)} = e^{-\sigma R} \tag{3.3}$$

where is $\tau(R)$ the ratio between the detected power P(R) at the location R and the initially launched power P(S), and σ is the attenuation coefficient.

The attenuation coefficient is sum of two main parameters [32].

$$\sigma = \sigma_1 + \sigma_2 \tag{3.4}$$

The first parameter σ_1 is the sum of scattering and absorption loses and the second parameter σ_2 is the sum of loses due to scintillation. Parameter σ_2 will be investigated in section 3.2.3.5. The extinction coefficient σ_1 is the sum of four terms [32],

$$\sigma_1 = \alpha_m + \alpha_n + \beta_m + \beta_n \tag{3.5}$$

where:

- α_m is the molecular absorption coefficient, refers to the structure and the composition of the atmosphere,
- α_n is the absorption coefficient of the aerosols (fine solid or liquid particles) present in the atmosphere (ice, dust, smoke, etc.),
- β_m is the Rayleigh scattering coefficient resulting from the interaction of light with particles of size smaller than the wavelength,
- β_n is the Mie scattering coefficient which originates from aerosols, i.e., when the incident particles are of the same order of magnitude as the wavelength of the transmitted wave.

In the interested wavelengths, which are between 780 nm and 1550 nm, the dimensions of the particles in the atmosphere are same order or greater than the wavelength. As a consequence, due to the molecular (Rayleigh) scattering varies with λ^{-4}, atmospheric and aerosol absorption can be negligible. Therefore, aerosol (Mie) scattering dominates the total attenuation coefficient. Thus, we can reduce the equation (3.5) to

$$\sigma_1 = \beta_n \qquad (3.6)$$

The efficiency of Mie scattering will be largest for aerosols with diameters of the laser wavelength. This efficiency, however, becomes practically independent of λ as the aerosol diameter increases. The attenuation due to scattering is described with Kim model in section 3.2.3.2.1.

3.2.3.1.   ABSORPTION ATTENUATION

Under clear air conditions, attenuation occurs mainly due to the absorption by gaseous molecules. Atmospheric absorption results from the interaction between photons and atoms or molecules, which leads to the absorption of the incident photon and an elevation of the temperature. The absorption coefficient depends on the type of gas molecules and their concentration [33].

Molecular absorption is wavelength dependent, which results in atmospheric transmission windows. The important atmospheric molecules that have high absorption in the infrared band include H_2O, CO_2, O_3 and O_2. Because the size of the gaseous molecules is much smaller than the wavelength, scattering attenuation from the gaseous molecules is negligible. Usually the laser wavelengths are selected to fall inside atmospheric transmission windows, so absorption attenuation is negligible. Typically, commercial FSO systems operate in windows around 850nm and 1550nm. Since these wavelengths are also used in fiber optic communications, standard components can be used lowering cost. There are other transmission windows available in the ranges between 3-5μm and 8-14μm, but the availability of components in these wavelengths is limited and more expensive [34].

Most of the models neglect the absorption attenuation due to the small effect on total attenuation. In our work, this attenuation is automatically taken into account with the usage of the PCModWin program. Fig.2 shows the total transmittance clean air in Ankara conditions. At the same time, the atmospheric windows that have been mentioned above can be also observed.
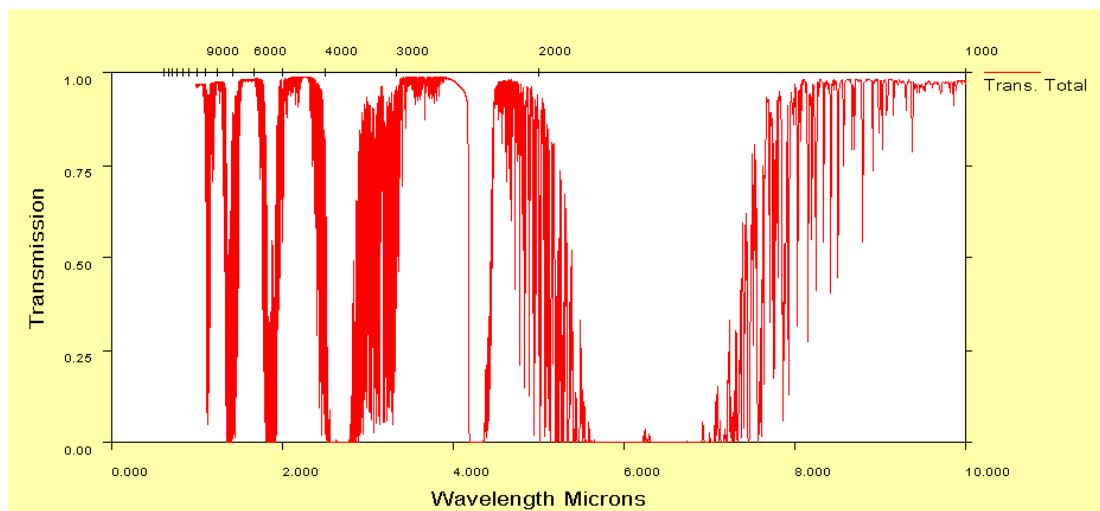
Figure 2 Transmittance as a Function of Wavelength Between 0-10μm in Clear Air with 1 km Range

3.2.3.2. SCATTERING ATTENUATION

Scattering attenuation caused by the presence of fog, mist, haze, drizzle, rain and snow particles. The presence of these particles causes an angular redistribution of the incident flux, known as scattering and reduces the flux propagation in the original direction.

Fig.3 shows the size parameters of atmospheric scattering particles for laser wavelengths of 785 nm and 1550 nm. In addition, corresponding regions for Rayleigh, Mie and non-selective or geometric scattering are plotted. For each type of scattering, the approximate relationship between the particle size and wavelength, and the wavelength power law of the attenuation coefficient is shown [10].

Rayleigh scattering occurs when the atmospheric particles are smaller than the wavelength. For the laser wavelengths of interest (785 nm and 1550 nm), Rayleigh scattering occurs due to the gaseous molecules in the atmosphere.
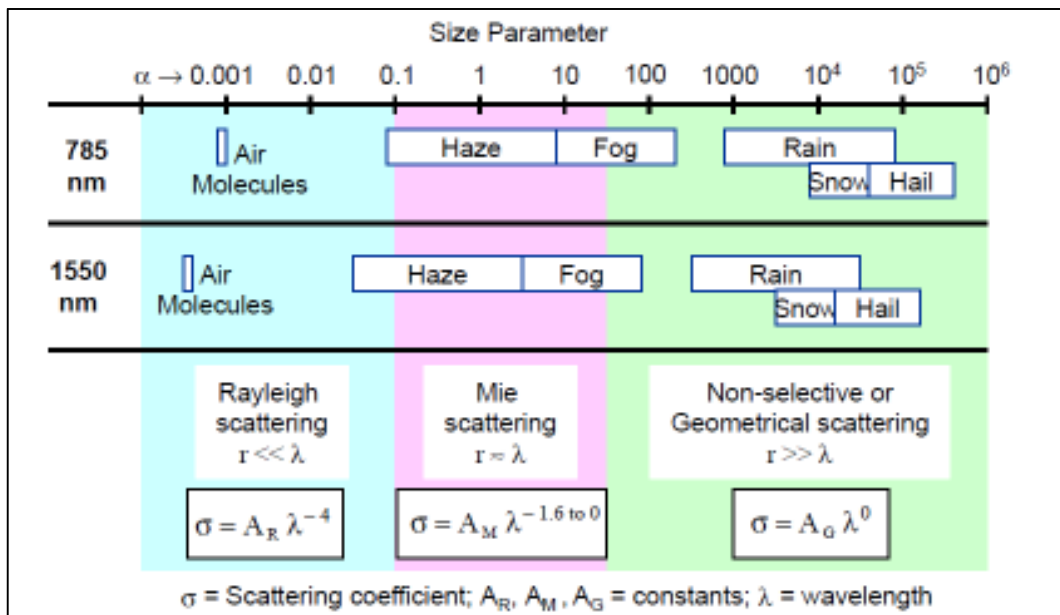
Figure 3 Size Parameters for Atmospheric Particles [10]

The Rayleigh attenuation coefficient varies as λ^{-4}. Thus, the effect of Rayleigh scattering on the total attenuation coefficient is very small and negligible.

For particles that are much larger than the wavelength, scattering can be described by geometric optics, which is independent of laser wavelength. Raindrops, snow, hail, cloud droplets and heavy fog will geometrically scatter laser light. For particles whose size is comparable to the laser wavelength, Mie scattering theory can be applied. Fog and aerosol particles are the major contributors to the Mie scattering attenuation. To compute the Mie scattering attenuation, FSO community has adopted some empirical methods in which, the attenuation coefficient due to Mie scattering is related to visibility.

3.2.3.2.1.   KRUSE AND KIM MODEL

Since an analytical approach is often not practical to compute the attenuation due to Mie scattering, empirical methods have been adopted by the FSO community. In these methods, the attenuation coefficient due to Mie scattering is related to visibility.

The technical definition of visibility or visual range is the distance that light decreases to 2% of the original power or qualitatively visibility is the distance at which it is just possible to distinguish a dark object against the horizon. The visibility parameter is easily measured and stored in meteorological stations or airports databases, which allows geo-local performance evaluation of these telecommunication systems using the distribution of this parameter. However, the visibility data collected at airports may not necessarily represent conditions found in either urban or rural environments, which can be very different in terms of topography and proximity to water [35].

An empirical simplified formula, which has been used in the FSO community to calculate the specific attenuation due to fog [10],

$$\beta_a = \frac{3,91}{V}\left(\frac{\lambda}{550nm}\right)^{-q} \tag{3.7}$$

where;

V is visibility in km

λ is wavelength in nm

q is
- 1.6 For high visibility (V > 50km)
- 1.3 For average visibility (6 km < V < 50 km)
- 0.16V+0.34 for haze visibility (1 km < V < 6 km)
- V-0.5 for mist visibility (0.5 km < V < 1 km)
- Zero for fog visibility (V < 0.5 km)

For visibility less than 500 m, the Kim model shows that there is no wavelength dependence for attenuation [36]. This means, unlike with absorption, a particular wavelength cannot be chosen to minimize or eliminate the effects of the Mie scattering due to its insensitivity to wavelength at low visibilities. It is also observed in Fig.4, which is a PCModWin plot of transmittance with 0,2 km visibility conditions at 0,2 km range without molecular absorption and precipitation. Transmission rate is almost stable between 0,5 micron to 2 micron wavelengths.
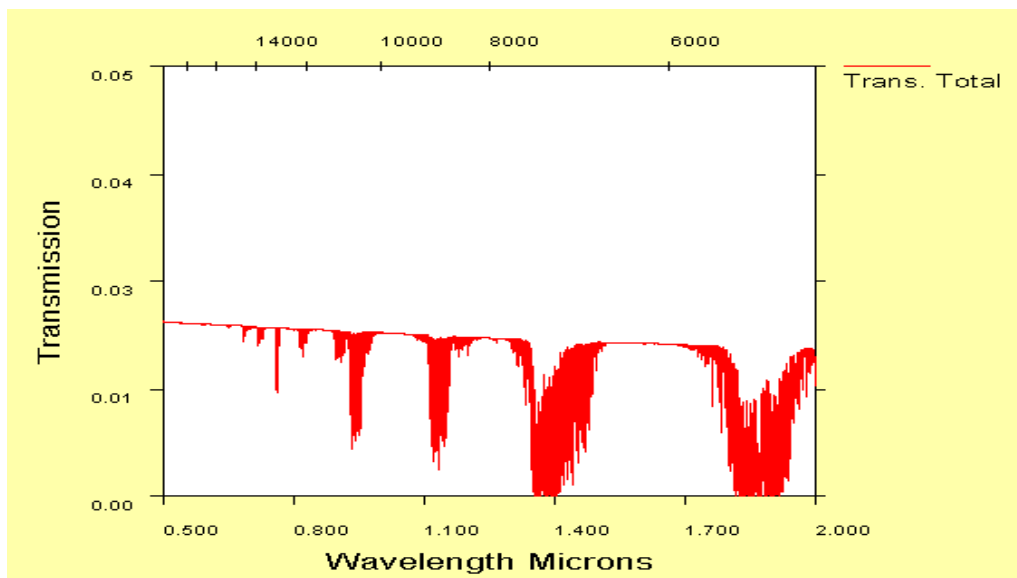
Figure 4 Transmittance Plot of 0,2 km Link in 0,2 km Visibility with PCModWin

A comparison between Kim model attenuation and PCModWin attenuation with a 0,5km visibility condition is shown in Fig.5.
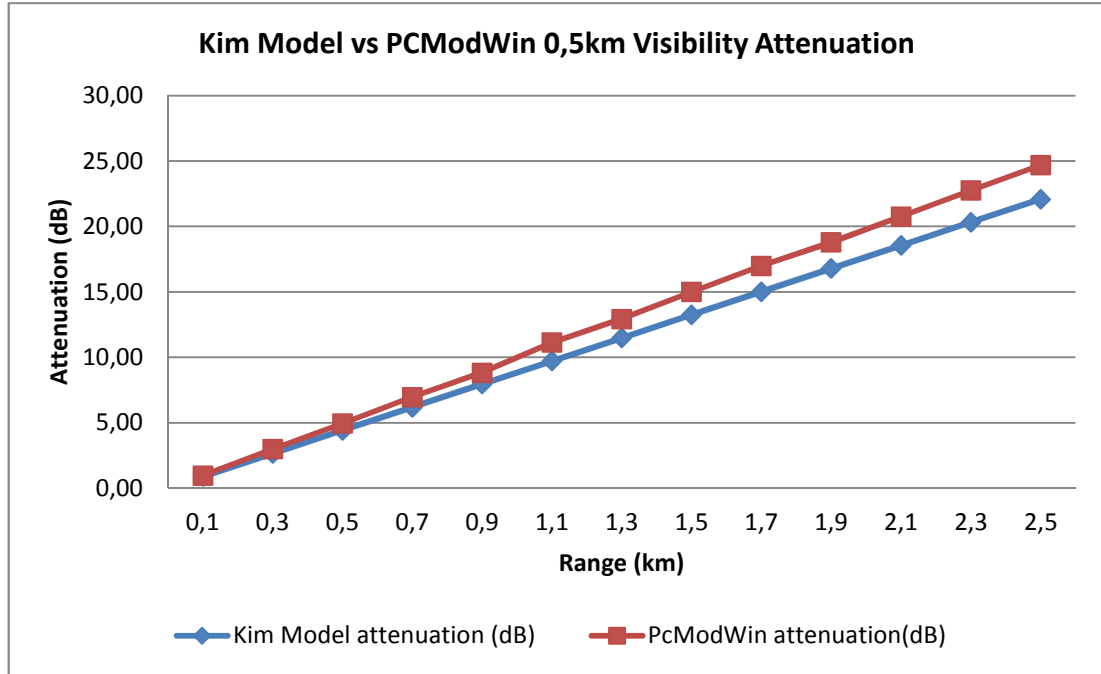
Figure 5 A Comparison between Kim Model and PCModWin Results.

3.2.3.3. RAIN ATTENUATION

Attenuation due to rain, independent of the wavelength, is a function of the precipitation intensity R (mm/h) according to the following relation [1]

$$L_{RAIN} = 1,076 \times R^{0,67} dB / km \qquad (3.8)$$

where, R is precipitation intensity (mm/h).

In our analysis, PCModWin transmittance values were used instead of modeling the attenuation. In international visibility code, precipitation is defined as light, moderate and heavy. According to meteorological authorities, we consider rain rate up to 2,5 mm/h as light rain, between 2,5 and 5 mm/h as moderate rain and at last 5 mm/h and over as heavy rain [37]. In Fig.6, a comparison between PCModWin simulation and

the Carbonneau model calculation given with Eq.3.8 is seen. As it can be seen, PCModWin attenuation has higher values. A worst condition scenario can be handled with these values.
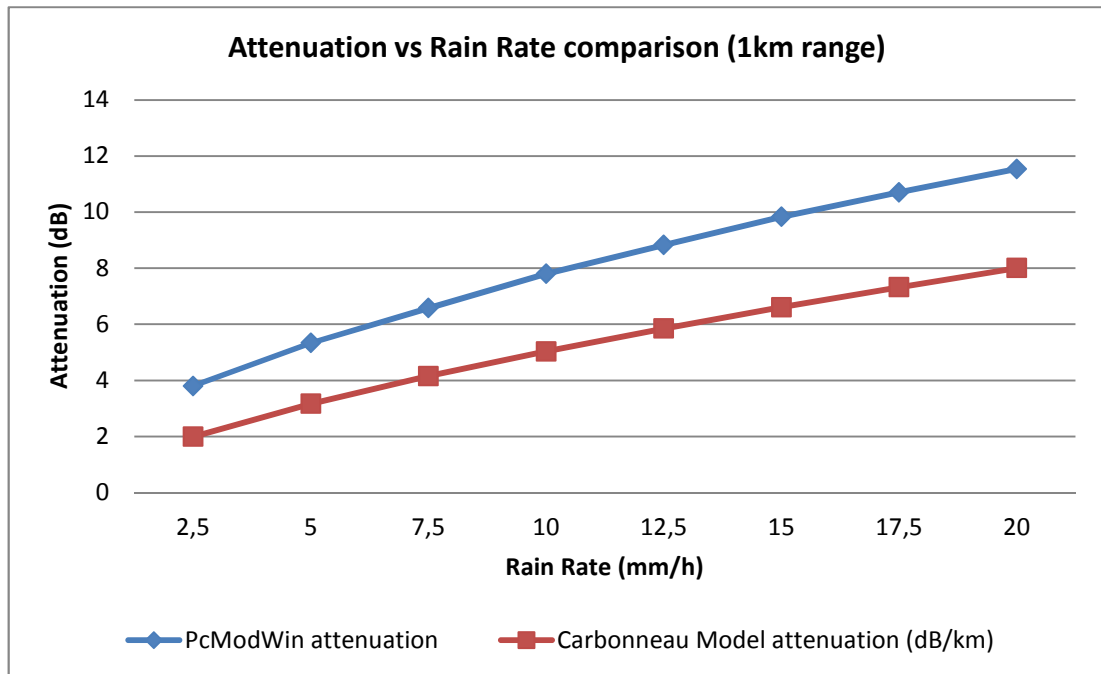
Figure 6 A comparison between Carbonneau Rain Attenuation Model and PCModWin Results

3.2.3.4.   SNOW ATTENUATION

Attenuation due to snow is a function of the wavelength λ (nm) and precipitation intensity S (mm/h) according to the following relations:

$$L_{SNOW} = a \times S^b \tag{3.9}$$

$$a = 5,42.10^{-5}\lambda + 5,4958776 \qquad b = 1,38 \tag{3.10}$$

$$a = 1,023.10^{-4}\lambda + 3,7855466 \qquad b = 0,72 \tag{3.11}$$

The attenuation due to snowfall has been modeled based on dry or wet snows and the specific attenuation is given by equation (3.9) where S is the snow rate in [mm/h].

The Parameters a and b are given for dry snow in equation (3.10) and for wet snow in equation (3.11). Fig.7 depicts the difference between wet and dry snowfall.
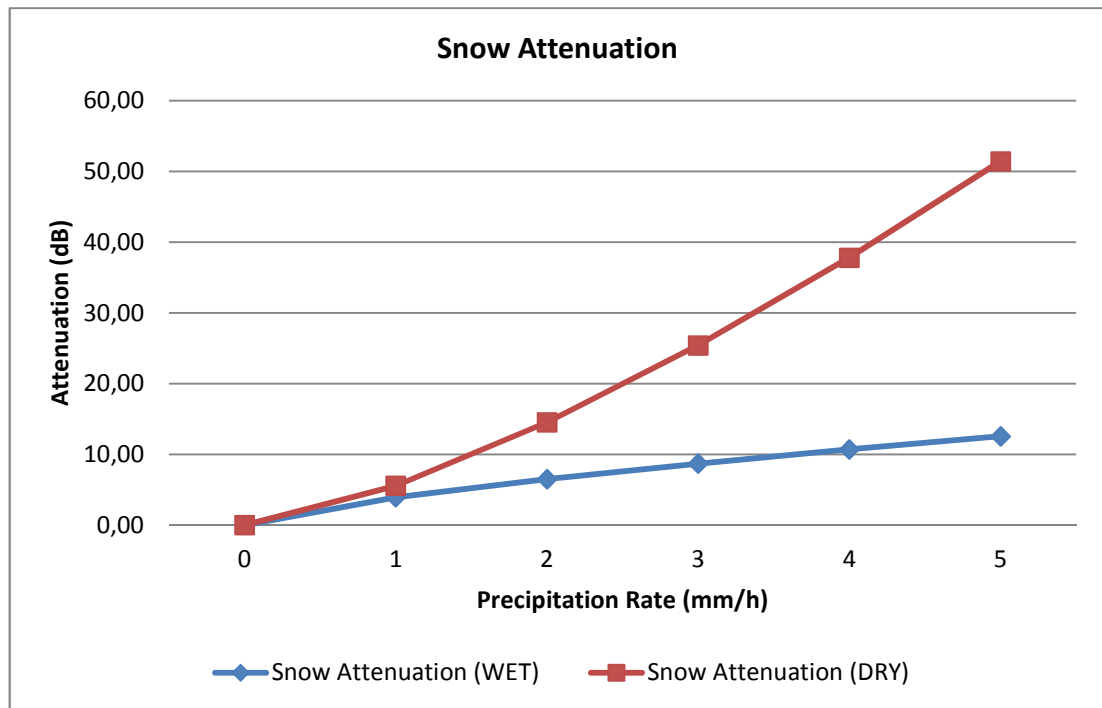
Figure 7 Wet and Dry Snow Attenuation versus Snow Rate.

3.2.3.5. TURBULENCE ATTENUATION

The most important effects of atmospheric turbulence on the laser beam are beam broadening, beam wander and redistribution of intensity within the beam, known as scintillation. In the case of strongly divergent beam, scintillation is the most significant source causing a loss of power.

There exist a few physical descriptions of turbulence attenuation. The Rytov approximation [38] and Andrews's method [39] are currently used in technical practice. We used Rytov approximation in this study.

On the basis of Rytov's analysis, the relationship between refractive index structure parameter C_n^2, which characterizes the volume of atmospheric turbulence (we

assume constant C_n^2 and low turbulence), and relative variance of optical intensity $\sigma_{I,rel}^2$ was set by Rytov as [40]

$$\sigma_{I,rel}^2 = K.C_n^2 k^{7/6} L^{11/6} \qquad (3.12)$$

where K is the constant 1,23 for the plane wave, and 0,5 for the spherical wave, C_n^2 is the refractive index structure parameter (m$^{-2/3}$), k presents the wave number (m^{-1}) and L signifies the distance (m) between the transmitter and receiver of the optical wireless link. Equation (3.12) holds true for

$$\sigma_{I,rel}^2 < 1 \qquad (3.13)$$

In technical reports and specialized publications turbulence attenuation is frequently given by the structure parameter of the refractive index of atmospheric transmission medium but the method of calculation is not specified. In every case, it is necessary to mention the method applied for the calculation of turbulence attenuation. Due to its acceptance by ITU and providing the worst condition according to comparison in [40], in our study, following relation was used [35].

$$\sigma_X^2 = 23,17 C_n^2 k^{7/6} L^{11/6} \qquad (3.14)$$

According to [16] and [40], scintillation peak-to-peak amplitude is equal to $4\sigma_\chi$ and attenuation related to scintillation is equal to $2\sigma_\chi$. Thus, the relation for turbulence attenuation L_{RYTOV} can be written as [32][40],

$$L_{RYTOV} = 2\sqrt{23,17 C_n^2 k^{7/6} L^{11/6}} \qquad (3.15)$$

In this equation, the most significant parameter is C_n^2. To evaluate C_n^2 we chose the macroscale meteorology semi-empirical model in our study. This model is based on the concept of temporal hours or a relative part of the day and is a reliable way to predict C_n^2 [41].

According to macroscale model, the value of C_n^2 is related strongly to the hour of the day. It has high values at noon and low values near sunrise and sunset. Accordingly, a concept of temporal hours *(th)* has been developed. The duration of one *th* is obtained by subtracting the hour of sunrise from that of sunset and dividing by 12. The current *th* is obtained by subtracting the hour of sunrise from the current hour and dividing by the value of one *th*. Therefore, at sunrise *th*=00:00h, at sunset *th*=12:00h, and at noon *th*=06:00h. Using this concept, a weight function was constructed whereby for each temporal hour, a normalized weight was specified and the weight vector was included in the regression model that describes C_n^2 according to the weather. The shape of the weight function was constructed by averaging C_n^2 data from many different meteorological conditions. The model for C_n^2 is

$$C_n^2 = 3,8 \times 10^{-14} W + 2 \times 10^{-15} T - 2,8 \times 10^{-15} RH + 2,9 \times 10^{-17} RH^2 - 1,1 \times 10^{-19} RH^3$$
$$- 2,5 \times 10^{-15} WS + 1,2 \times 10^{-15} WS^2 - 8,5 \times 10^{-17} WS^3 - 5,3 \times 10^{-13} \qquad (3.16)$$

where W is the temporal-hour weight, which is described in appendix, T is the air temperature (K), RH is the relative humidity (%), and WS is the wind speed (ms $^{-1}$). This model for C_n^2 applies about 15 m elevation. Dynamic range for temperature is from 9 to 35 degree Celsius, for relative humidity from %14 to %92 and for wind speed from 0 to 10 m/sec.

Elevations over than 15 m, the calculated value of C_n^2 can be scaled according to various models of the height profiles. Although many models have been suggested, experiments described in [42] for measurements up to 100-m elevation support primarily the model of Tatarskii [43] which gives

$$C_n^2(h) = C_{n0}^2 h^{-4/3} \qquad (3.17)$$

where C_{n0}^2 is the refractive-index structure coefficient at the surface. This height profile would no longer be valid at the boundary level. For our study, this height (100m) is high enough to model the link behavior.

In this thesis, C_n^2 values were calculated with Eq. 3.16 with the collected meteorological data for Ankara to see the changes during the day. As it can be seen in Fig.8 and Fig.9, values are increasing at noon and at sunrise and sun set C_n^2 has the lowest values as expected.
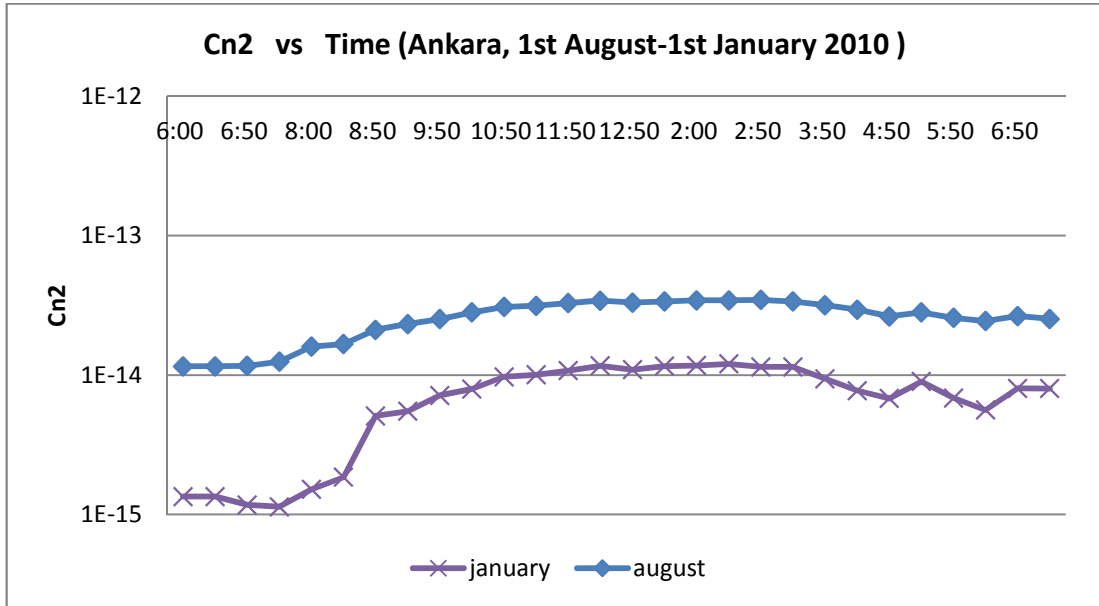
Figure 8 Change of C_n^2 During Day in Ankara (01.01.2010 and 01.08.2010)
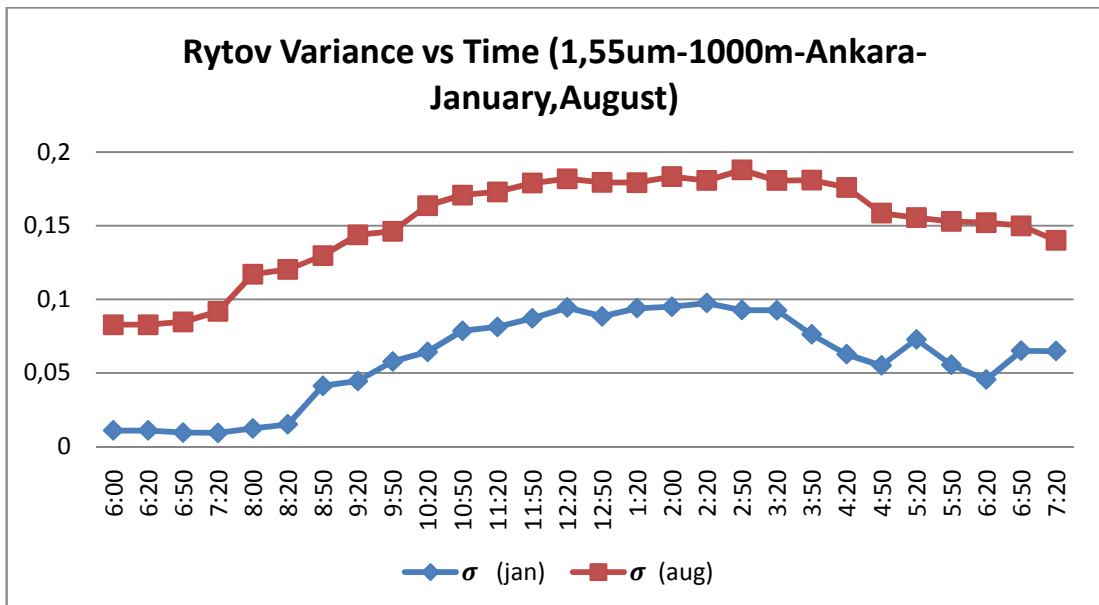
Figure 9 Change of $\sigma_{I,rel}^2$ During Day in Ankara (01.01.2010 and 01.08.2010)

In Fig.10, scintillation attenuation versus link distance for four different C_n^2 plots can be seen. In this study, due to the large number of samples, scintillation attenuation was not calculated for all cases. For our case-1 (1 km link) a 6dB margin and for case-2, a 12dB margin was considered for the worst C_n^2 value of 10^{-14}.
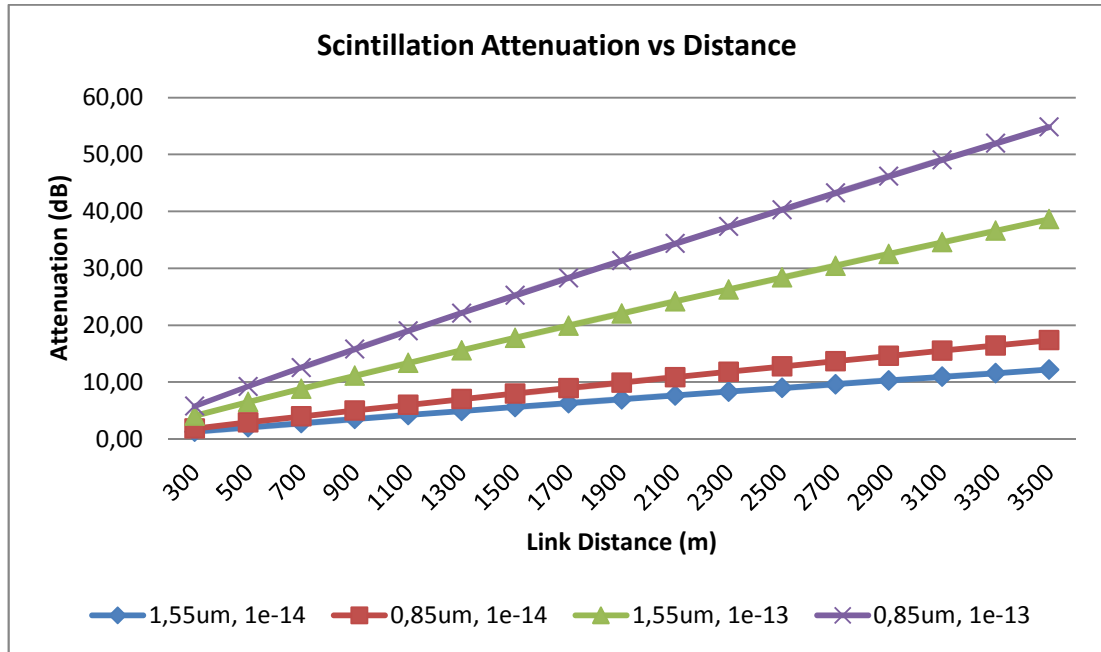
Figure 10 Scintillation Attenuation vs Distance Plot.

Turbulence can become very strong near the ground because of the heat transfer between ground and air. However, even at a modest height of 50 meters, which is used in the study, strong turbulence is rarely observed in various experiments. Nevertheless, strong turbulence can still occur if the beam propagates near rooftops and near other structures that cause increased temperature fluctuations (e.g. chimneys, air conditioners).

CHAPTER 4

LINK AVAILABILITY OF FSO SYSTEMS

One of the most important things to know in free space optical communication is the availability of the laser link. When a link is installed, mathematical models allow the availability calculation of the link for one year or for the most unfavorable month with the system parameters that are provided by manufacturers. For commercially available FSO systems, certain bit error rate (BER) and availability values are often specified, but the measurement period and the measurement sites are not mentioned. However, they must be specified, because all parameters may change during the year depending where the FSO link will be installed. In our study, link availability values for commercially available FSO systems are investigated. Beside mathematical models, also computer simulations (PCModWin-MODTRAN) were used to get more accurate result. In this chapter;

- The meteorological data that was used in calculations,
- Informatıon about the PCModWin (MODTRAN) software that was used to obtain atmospheric attenuation values,
- Manufacturer data, which provides parameters for simulations and calculations,
- Availability model that was used in this study will be given.

4.1. METEOROLOGICAL DATA

In our study, we chose three largest cities of Turkey to perform link availability calculations due to more detailed available meteorological data. In Turkey, "Turkish State Meteorological Service" provides meteorological data but the historical data is closed to public usage. Thus, meteorological data that was used in our study was obtained from the website of Weather Underground Company [44]. This website provides the historical meteorological data that we need in our study beside a huge amount of meteorological data, analysis and forecasts. In this site, international current conditions are collected directly from more than 8,000 weather stations located in countries around the globe. Typically these stations are owned by government agencies and international airports and data is updated at 0.5,1, 3, or 6 hour intervals, depending upon the station.

Due to accessibility to more detailed historical data, three biggest airports of Turkey were chosen to get the meteorological data. Esenboğa (LTAC) data for Ankara, Ataturk (LTBA) data for İstanbul and Adnan Menderes (LTBJ) data for İzmir were used. In these stations' reports, temperature, humidity, pressure, visibility and precipitation data are given with a 30 minutes interval. An example table is shown at table 1.

Table 1 Meteorological Data of İzmir Adnan Menderes Airport on 25 March 2010

Time (EET)	Temp.	Humidity	Pressure	Visibility	Wind Speed	Conditions
12:20 AM	**12.0** °C	88%	**1014** hPa	**10.0** km	**13.0** km/h / **3.6** m/s	Mostly Cloudy
12:50 AM	**11.0** °C	88%	**1014** hPa	**10.0** km	**13.0** km/h / **3.6** m/s	Mostly Cloudy
1:20 AM	**11.0** °C	88%	**1014** hPa	**10.0** km	**11.1** km/h / **3.1** m/s	Mostly Cloudy
1:50 AM	**11.0** °C	88%	**1014** hPa	**10.0** km	**11.1** km/h / **3.1** m/s	Mostly Cloudy
2:00 AM	**11** °C	86%	**1014** hPa	**15** km	**11.1** km/h /	Partly Cloudy
2:20 AM	**11.0** °C	88%	**1014** hPa	**10.0** km	**13.0** km/h / **3.6** m/s	Mostly Cloudy
2:50 AM	**11.0** °C	88%	**1014** hPa	**10.0** km	**13.0** km/h / **3.6** m/s	Mostly Cloudy
3:20 AM	**11.0** °C	88%	**1014** hPa	**10.0** km	**20.4** km/h / **5.7** m/s	Mostly Cloudy
3:50 AM	**10.0** °C	87%	**1014** hPa	**10.0** km	**16.7** km/h / **4.6** m/s	Mostly Cloudy

4.2.   MODTRAN

MODTRAN (MODerate resolution TRANsmission) is an atmospheric model developed over the past 25 years at the US Air Force Research Laboratory. It is the direct successor to the LOWTRAN family of codes; in fact, MODTRAN contains the complete LOWTRAN model as a user option. It can be used to calculate the transmission and the radiance for a specified path through the atmosphere. MODTRAN is useful as a stand-alone program; it is also implemented as a subroutine or separate module in many larger system codes. MODTRAN is written as a FORTRAN 77 program, and the full model source code is available to end users for a nominal distribution fee.

The MODTRAN transmission calculations use three temperature dependent parameters: an absorption coefficient, a line density parameter, and an average line width. The spectral region is partitioned into 1 cm^{-1} bin for each molecule. Within each bin, contributions from transitions whose line centers fall within the bin are molded separately from nearby lines centered outside the bin. The absorption due to lines within the bin is calculated by integrating over a Voigt line shape. The Curtis-Godson approximation, which is accurate for the moderate temperature variations in the earth's atmosphere, is used to replace multilayered paths by an equivalent single homogeneous one. Molecular continuum absorption, molecular scattering, and aerosol absorption and scattering are also included. The radiance calculations consider contributions from the following sources:

- atmospheric self-emission
- solar and/or lunar radiance single-scattered into the path
- direct solar irradiance through a slant path to space
- multiple scattered solar and/or atmospheric emitted radiance into the path

MODTRAN is valid over the spatial frequency range 0 to 50000 cm^{-1}, or for wavelengths longer than 0,2 micrometers. MODTRAN's maximum spectral resolution is 2 cm^{-1}; this spectral resolution is adequate for many tasks and is responsible for the name of the model.

4.2.1. PCModWin

In our study, we used PCModWin 4.0 v3r1 Version 1.4 for the calculation of the transmittance of the atmosphere. PCModWin provides a graphical environment in which to set up, run and manipulate model calculations made by the MODTRAN atmospheric code. The currently available version of MODTRAN (MODTRAN 4.0) is included in PCModWin.

In our work, scattering, absorption and precipitation attenuations were calculated with PCModWin software. Below, some example outputs for different scenarios are presented.
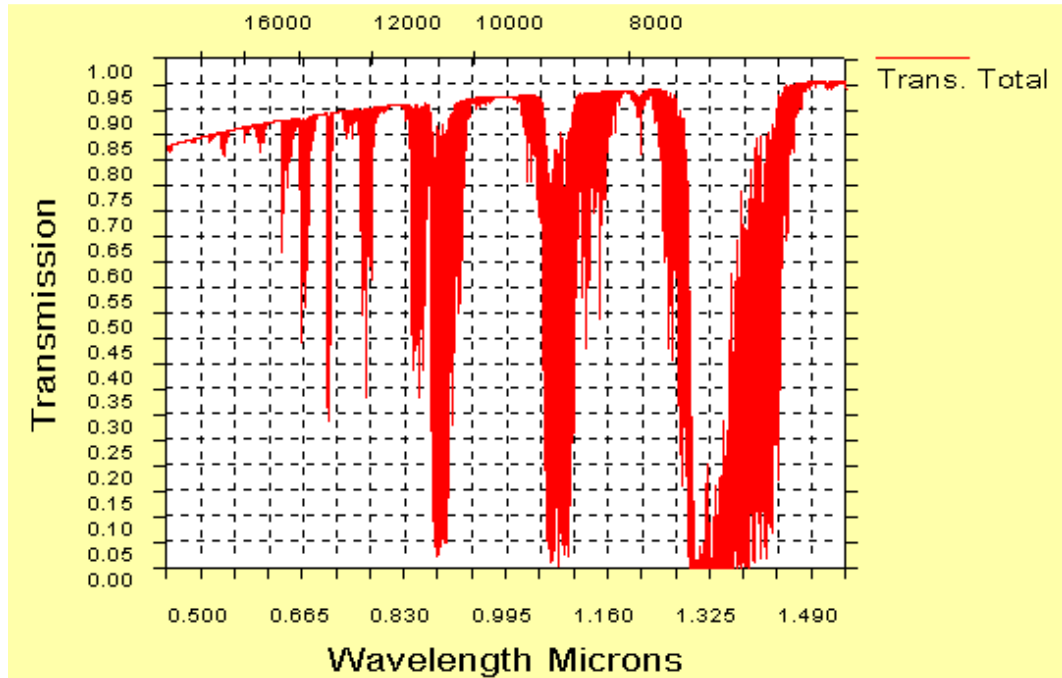
Figure 11 Transmission of 1km Link with 23km Visibility (Clear Air) and No Rain

In Fig.11, the atmospheric windows can be clearly seen. With a 23km visibility and without any precipitation, according to PCModWin the atmospheric attenuation of light at 850 nm is 0,45dB/km and at 1550 nm it is only 0,22 dB/km.

The severe effect of fog is seen in Fig.12. At 850 nm wavelength, the attenuation is almost 20dB/km and at 1550 nm, it is 10 dB/km. With this figure, the importance of wavelength selection can also be seen. In same conditions, 1550 nm has a 10dB advantage to 850 nm.
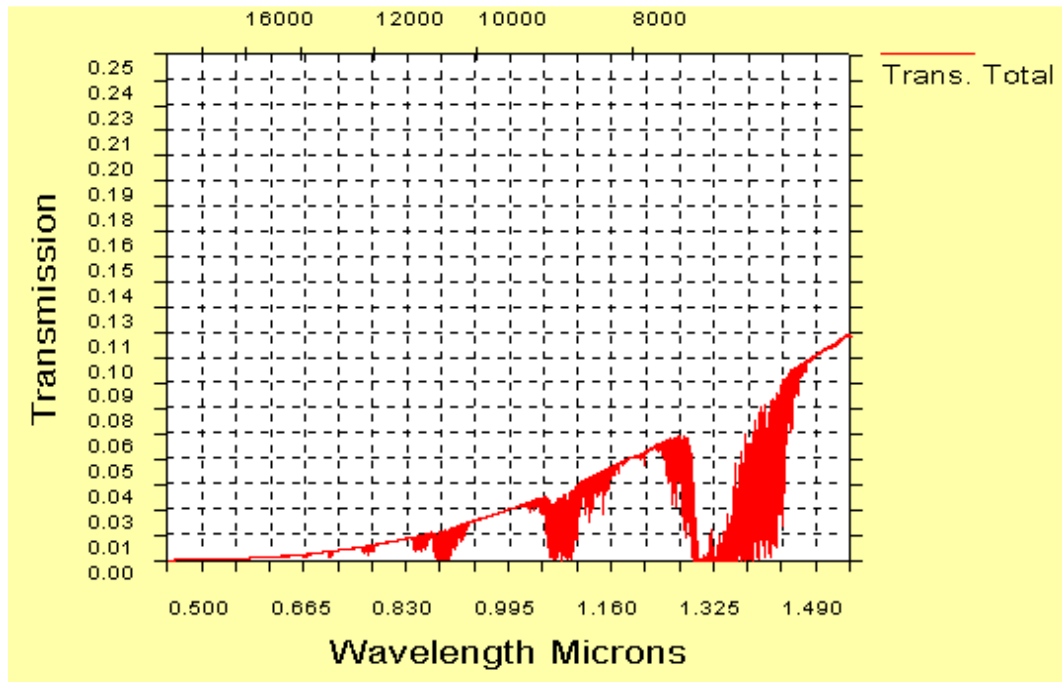
Figure 12 Transmission of 1km Link with 0,5km Visibility (Moderate Fog) and No Rain.

Heavy rain could be also a major effect on the link availability. In Fig.13, rain effects on the transmission of electromagnetic waves which are in 500nm-1600nm spectral range are shown. According to results, 12,5mm/h rain could cause 7dB attenuation. An attractive point, the attenuation at this spectral range is almost same at every wavelength. Thus, it can be said that rain attenuation is independent from wavelength at our interested range.
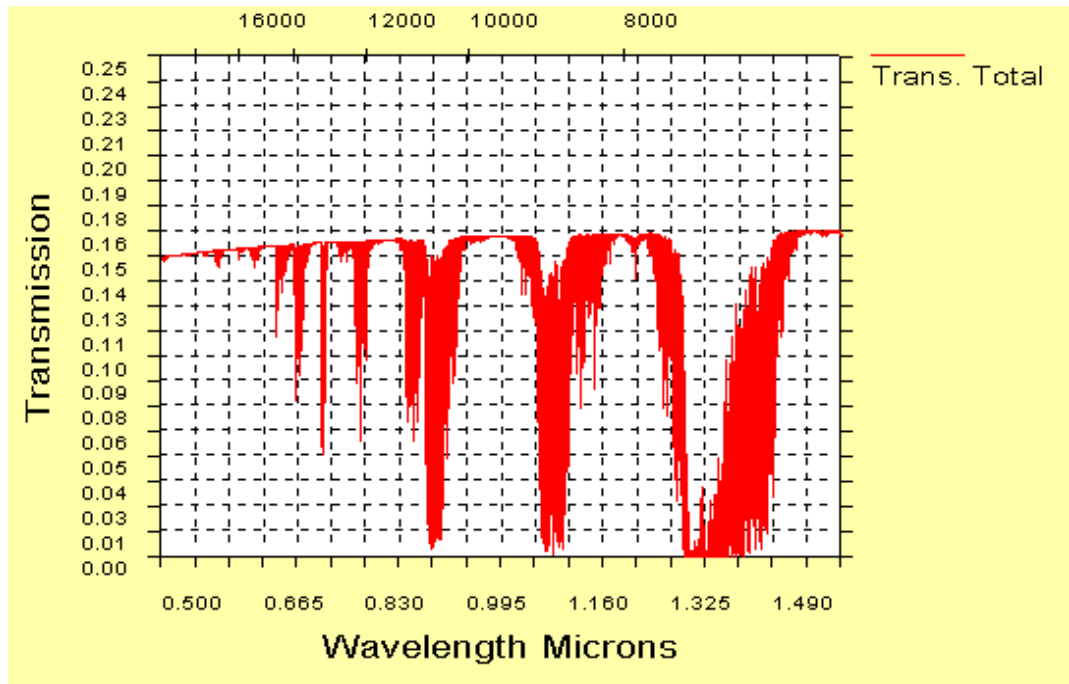
Figure 13 Transmission of 1km Link with 23km Visibility (Clear Air) and 12,5mm/h Rain (Heavy Rain).

4.3. MANUFACTURER DATA

Most of the system parameters are freely available from manufacturers' data sheets, but generally they are not detailed enough to make an availability calculation. Thus, a link budget comparison table from [45] AirFiber company's white paper was used.

Because of the proven superiority of 1550nm wavelength, only two highlighted products were considered, which have different transmit power and sensitivity values. In the calculations, vendor B and vendor C parameters were used. Both equipment Bit Error Rate (BER) is considered as 10^{-12} when the received signal is greater than the specified receive sensitivity value. Thus, we did not investigate the BER of the link. As long as we were within our link margin, it is considered that we had an acceptable BER value.

Table 2 Manufacturer Parameters of Some Commercial FSO Systems.

	VENDOR A	VENDOR B	VENDOR C	VENDOR A	
Transmitter	AlGaAs	AlGaAs	AlGaAs	AlGaAs	
Modulation Format	NRZ OOK	NRZ OOK	NRZ OOK	NRZ OOK	
Receiver	APD	APD	APD	APD	
Wavelength	850	1550	1550	850	nm
Range	190	215	205	176	m
Data Rate	1250	1250	155	1250	Mbit/s
Average Laser Power	30	1000	320	15,60	mW
Peak Laser Power	60	2000	640	31	mW
Transmit Aperture	5	16	2,50	5	cm
Transmit Divergence	2	2	4,25	2	mrad(1/e^2)
Receive Aperture	20	40	20	19	cm
Optical Background	0,2	0,2	0,2	0,2	W/m^2/nm/sr
Receiver FOV	3,25	3,25	3,25	3,25	mrad(1/e^2)
Receive Filter Width	25	25	25	25	nm
Receiver Sensitivity	1000	1000	1000	1000	nW
BER	1.00E-12	1.00E-12	1.00E-12	1.00E-12	
Peak Laser Transmit Power	-12,218	3,010	-1,938	-15,086	dBW
Atmospheric Scintillation Fade	-1	-1	-1	-1	dB
Receive Optics Attenuation	-1,4	-1,4	-1,4	-1,4	dB
Bandpass Filter Loss	-0,7	-0,7	-0,7	-0,7	dB
Misc Loss Elements	0	0	0	0	dB

4.4. LINK AVAILABILITY ANALYSIS

In this study, availability analysis of three biggest cities in Turkey was investigated. Meteorological data belongs to year 2010 was gathered from airport reports with a thirty minutes time interval. For availability analysis, two different commercial FSO equipment's parameters were used. To see the link distance effect, two cases were investigated.

In first case;

- Link distance was considered as 1km,
- Two manufacturers' parameters were used that is given in table 2,
- For rain and geometric attenuation, models that are described in ITU-R F.2106-1 were used,
- For atmospheric attenuation, PCModWin(MODTRAN) simulations were run,
- As site, Ankara, İzmir and İstanbul are studied.

In second case, link distance was considered 3 km and the other items were considered same with the first case.

4.4.1. LINK BUDGET CALCULATION

Link budget calculations were made as described in Eq. 3.1. An example link budget table for Ankara is given on table 3 and all stages of link budget calculation are explained systematically below.

- Hourly meteorological (Table 3) data was filtered according to its visibility and precipitation values and rearranged in an excel table.
- In rearranged table, the first column has the visibility value.
- In second and third columns, transmission rates which were obtained from PCModWin,
- In fourth column, number of the 30 minutes time intervals,
- In other columns, different attenuation values, which were calculated according to ITU-R F.2106-1, are given.
- After obtain the total attenuation values for both cases, according to sensitivity values of FSO systems, the total number of unavailable time intervals were calculated.
- Final, availability values can be simply calculated according to Eq. 4.1, which is given in availability calculation when we get the number of unavailable time.

Table 3 Link Budget Table for Ankara, January 2010.

	JANUARY				1km	3km	1km	3km	1km	3km	__	unavailable intervals
	1km	3km%										2	66
FSO-2	99,866%	95,565%										2	66
FSO-1	100,000%	97,446%										0	38
31	1488	1488			1km	3km	1km	3km	1km	3km	1km	3km
visibilty	1550-1	1550-3			precip.	precip	Geo	Geo	Sys+Scin	Sys+Scin	total-1	total-3
0,2	0,0034	0,000001	2	clear	0	0	15,56	24,08	10	18	50,245211	102,08
0,3	0,034	0,00001	2	clear	0	0	15,56	24,08	10	18	40,245211	92,08
0,4	0,058	0,0002	13	clear	0	0	15,56	24,08	10	18	37,92572	79,0697
0,5	0,104	0,001	8	clear	0	0	15,56	24,08	10	18	35,389667	72,08
0,6	0,147	0,0032	1	clear	0	0	15,56	24,08	10	18	33,886827	67,0285
0,7	0,197	0,0073	4	clear	0	0	15,56	24,08	10	18	32,615338	63,446771
0,8	0,243	0,0136	3	clear	0	0	15,56	24,08	10	18	31,703937	60,744611
0,9	0,282	0,0244	8	clear	0	0	15,56	24,08	10	18	31,057509	58,206102
1	0,317	0,035	2	moderate	4,4	13,2	15,56	24,08	10	18	34,949407	69,83932
1,3	0,413	0,091	2	clear	0	0	15,56	24,08	10	18	29,400499	52,489586
1,6	0,49	0,124	4	clear	0	0	15,56	24,08	10	18	28,658039	51,145783
1,6	0,49	0,124	3	light	2,83	8,49	15,56	24,08	10	18	31,488039	59,635783
1,6	0,49	0,124	4	moderate	4,4	13,2	15,56	24,08	10	18	33,058039	64,345783
1,7	0,513	0,139	1	clear	0	0	15,56	24,08	10	18	28,458826	50,649852
1,7	0,513	0,139	1	moderate	4,4	13,2	15,56	24,08	10	18	32,858826	63,849852
1,8	0,536	0,151	1	clear	0	0	15,56	24,08	10	18	28,268352	50,290231
1,9	0,551	0,176	1	clear	0	0	15,56	24,08	10	18	28,148484	49,624873
1,9	0,551	0,176	2	light	2,83	8,49	15,56	24,08	10	18	30,978484	58,114873
2	0,564	0,182	11	clear	0	0	15,56	24,08	10	18	28,047209	49,479286
2	0,564	0,182	2	light	2,83	8,49	15,56	24,08	10	18	30,877209	57,969286
2	0,564	0,182	4	moderate	4,4	13,2	15,56	24,08	10	18	32,447209	62,679286
2,1	0,578	0,197	2	light	2,83	8,49	15,56	24,08	10	18	30,770722	57,625338
2,2	0,591	0,211	2	clear	0	0	15,56	24,08	10	18	27,844125	48,837175
2,2	0,591	0,211	1	light	2,83	8,49	15,56	24,08	10	18	30,674125	57,327175
2,2	0,591	0,211	1	moderate	4,4	13,2	15,56	24,08	10	18	32,244125	62,037175
2,3	0,607	0,229	1	moderate	4,4	13,2	15,56	24,08	10	18	32,128113	61,681645
2,4	0,616	0,241	3	clear	0	0	15,56	24,08	10	18	27,664193	48,25983
2,5	0,637	0,255	6	clear	0	0	15,56	24,08	10	18	27,518606	48,014598
2,5	0,637	0,255	4	light	2,83	8,49	15,56	24,08	10	18	30,348606	56,504598
2,5	0,637	0,255	1	heaviy	5,62	16,87	15,56	24,08	10	18	33,138606	64,884598

4.4.2. AVAILABILITY CALCULATION

Availability of a link is given by formula;

$$\delta = \frac{\tau_{total} - \tau_{un}}{\tau_{total}} \tag{4.1}$$

where δ is availability, τ_{total} is total sampling time and τ_{un} is total unavailable time. For example, according to table 3, there are 38 unavailable time intervals for case-2 and FSO-1. Calculation of availability for this example is given below.

$$\tau_{tot} = 24 \text{ x } 31 \text{ x} 2 = 1488 \text{ (30 min intervals)} \qquad (4.2)$$

$$\tau_{un} = 38 \text{ (Total loss is higher than 63dB)} \qquad (4.3)$$

$$\delta = \frac{1488 - 38}{1488} = \%97.446 \qquad (4.4)$$

Same calculation was performed for all year and all cities. As a result, relation between the weather conditions and the availability was investigated.

CHAPTER 5

ANALYSIS

All researches and experiments about FSO show that fog is the most severe factor that reduces the availability of the link. According to Turkish State Meteorological Service, maximum numbers of foggy days are seen in Central Anatolia and the minimum numbers are seen in Mediterranean. Even with this data we can guess that Ankara will have the worst availability values.

First, visibility values were investigated for all cities. As it was mentioned, Ankara has the worst conditions. Graphs for the most unfavorable months are given in Fig.14 and Fig.15.
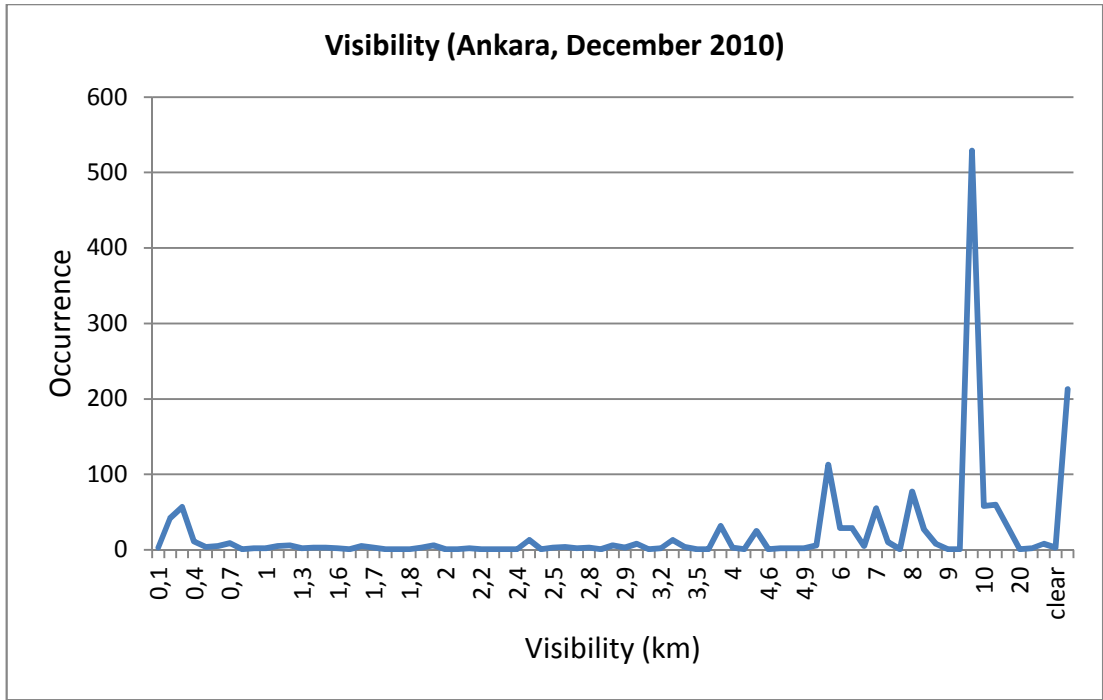
Figure 14 Visibility-Occurrence Graph of Ankara for the Most Unfavorable Month.

As it seen from the Fig.14 and Fig.15, in Ankara, the visibility values are lower than İzmir and İstanbul. In addition, the occurrence of the low visibility is higher than other cities. In 2010 the visibility was below 1 km in Ankara along 123,5 hours, in İzmir along 24 hours and in İstanbul along 26 hours. On the other hand, in Ankara 8375 hours, in İzmir 8665 hours and in İstanbul 7313 hours long the visibility was over 10km.
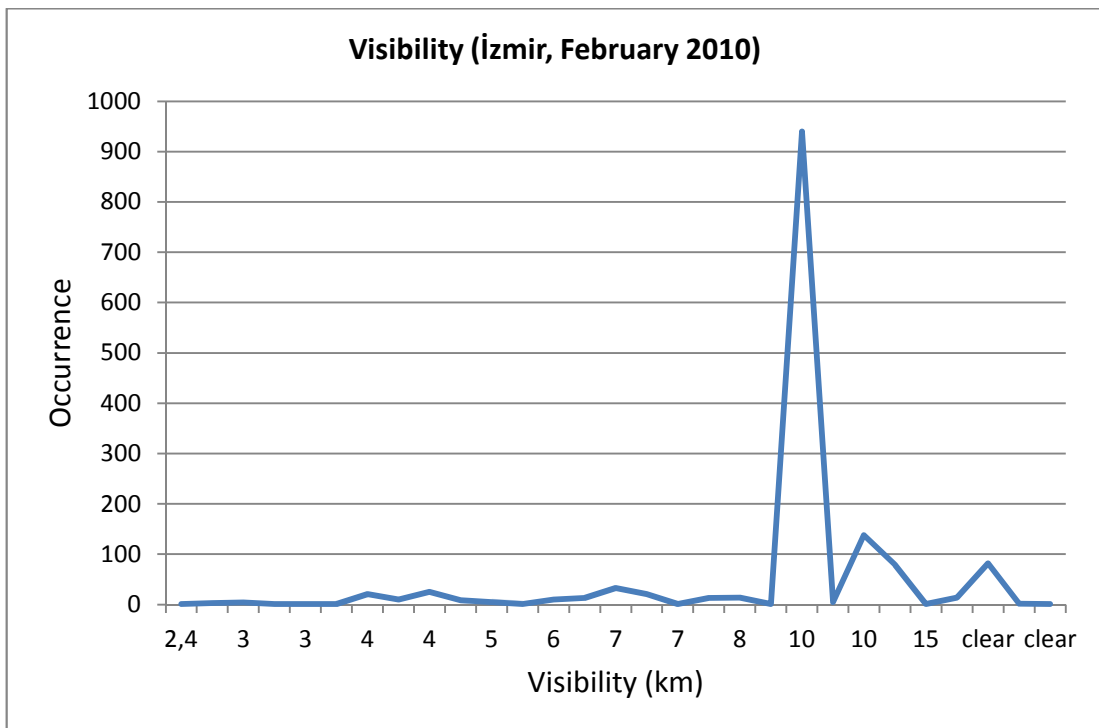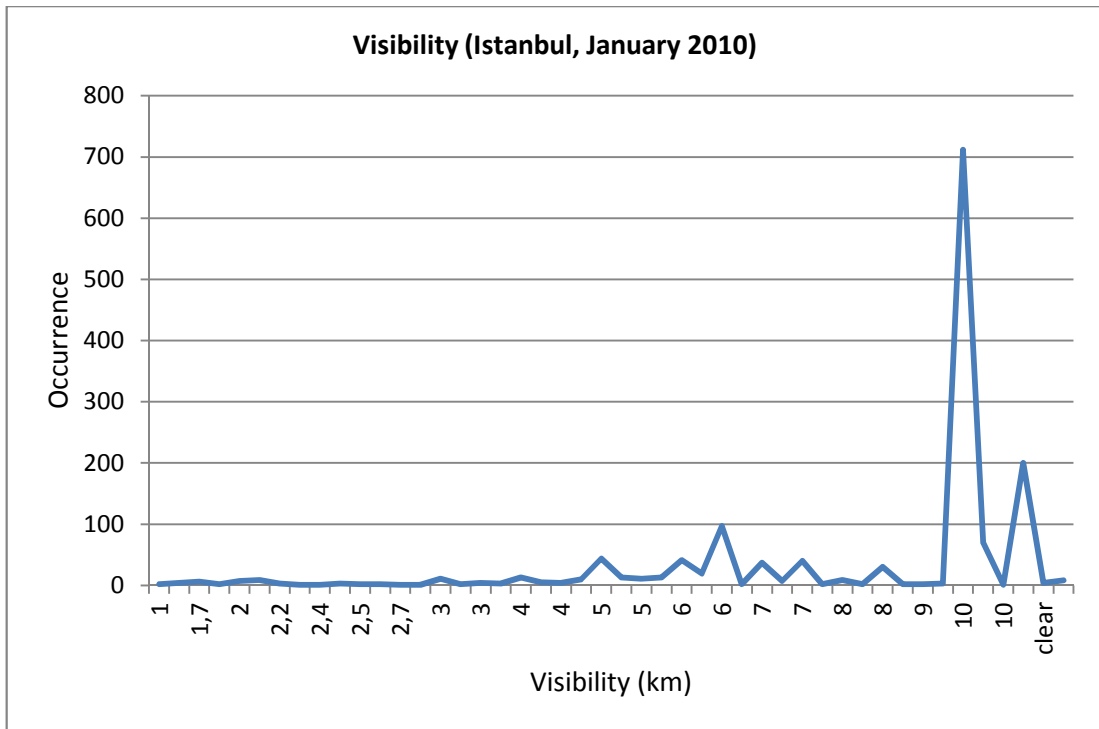
Figure 15 Visibility Graphs of İstanbul and İzmir for the Most Unfavorable Months.

On the other hand, even in the most unfavorable month, the visibility in İzmir did not go below 2,4km.Rain attenuation made this month the most unfavorable for İzmir. In

2010, along 520,5 hours moderate and over precipitation has occurred In İzmir. This value was 429,5 hours in Ankara and 843 hours in İstanbul.

Only with statistics of the visibility and precipitation occurrence frequency, it could be said that İzmir is advantageous with both visibility and precipitation. Although İstanbul has more rainy hours than Ankara, the huge difference between the total numbers of foggy hours, which is the major effect of link attenuation, make Ankara the worst appropriate city to install an FSO link.

To see which effect is most responsible from the attenuation, cumulated link budget tables for the worst months were plotted and given in Fig.16-18.
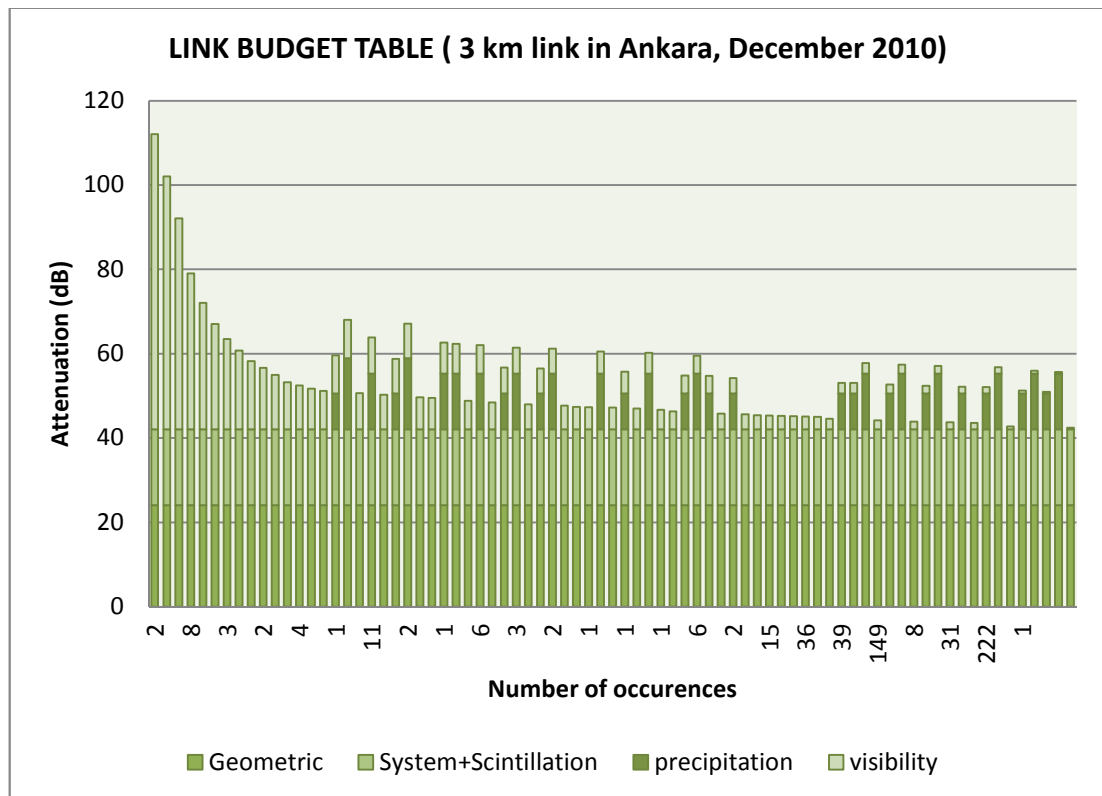

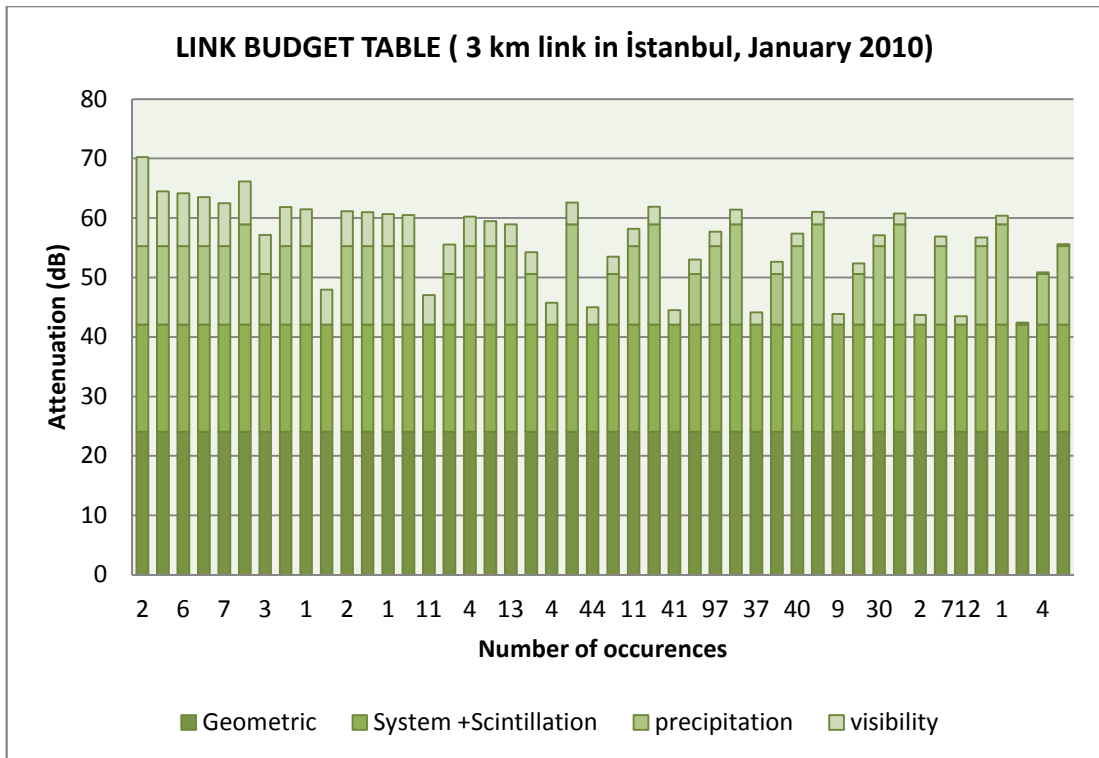**Figure 16** Link Budget Table for Ankara, December 2010

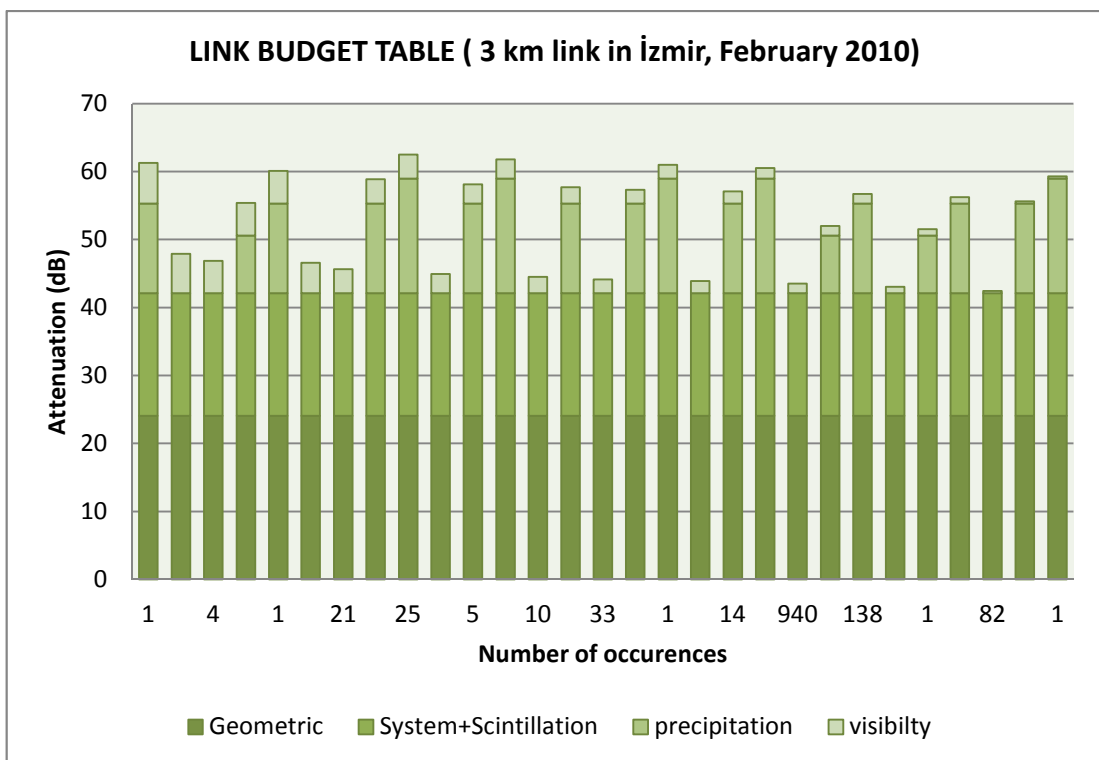**Figure 17** Link Budget Table for İstanbul, January 2010

Figure 18 Link Budget Table for İzmir, February 2010

When we investigate the link budget tables, out of constant losses (geometric, system and scintillation), generally precipitation losses take the first place. In İzmir and İstanbul, this rule can be generalized for all year long but in Ankara, fog is the major effect in the winter. It is known that fog effect is more severe than rain effect. Thus, it is expected that FSO links should be more available in İzmir and İstanbul. In addition, it is observed that Ankara experienced the highest attenuation values. In Fig.19, attenuation analyses for the most unfavorable months of all three cities are shown. The severe effect of fog to the total attenuation can be easily observed in Ankara while precipitation effect had larger part than visibility effect in İstanbul and in İzmir.
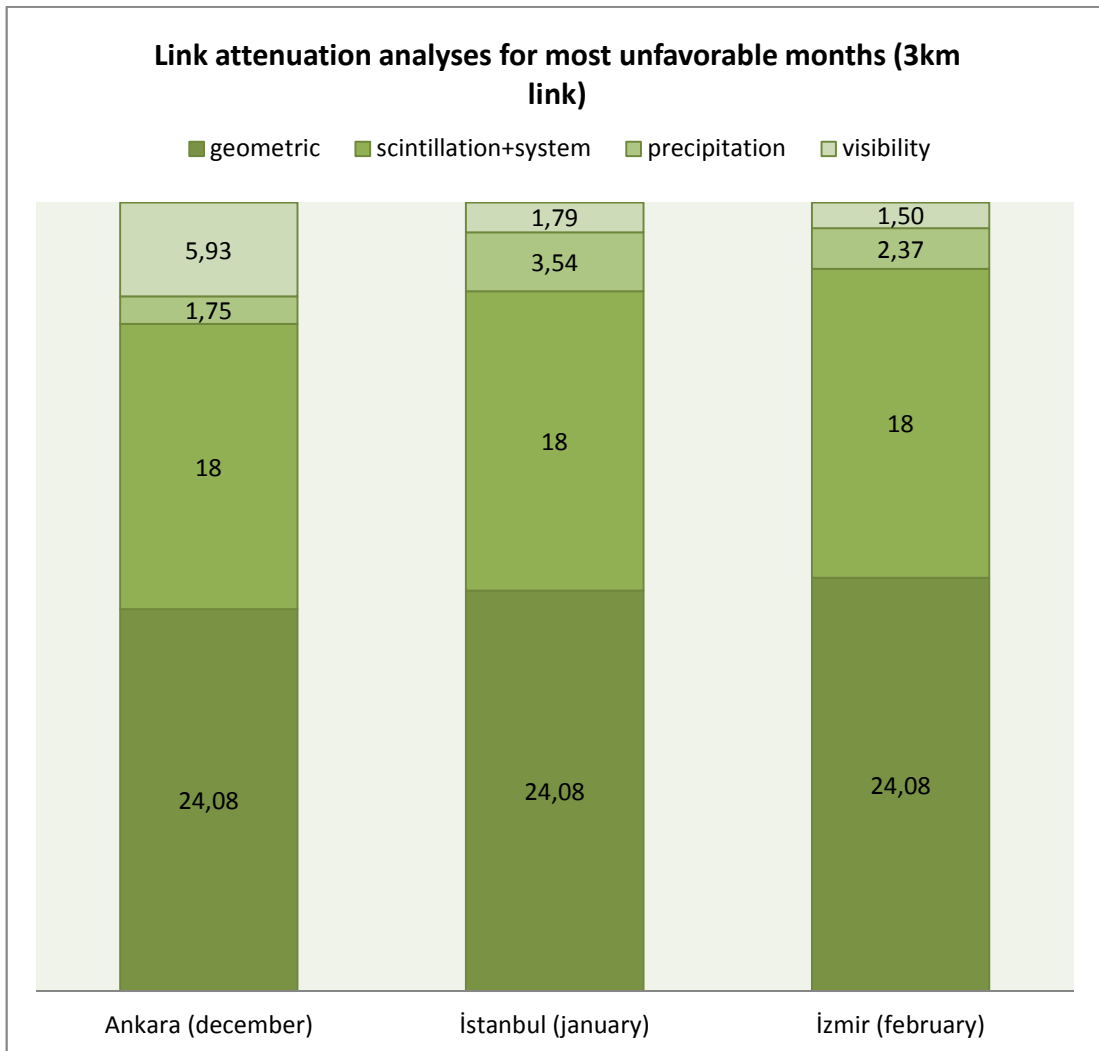

Figure 19 Attenuation Analyses for the most Unfavorable Months

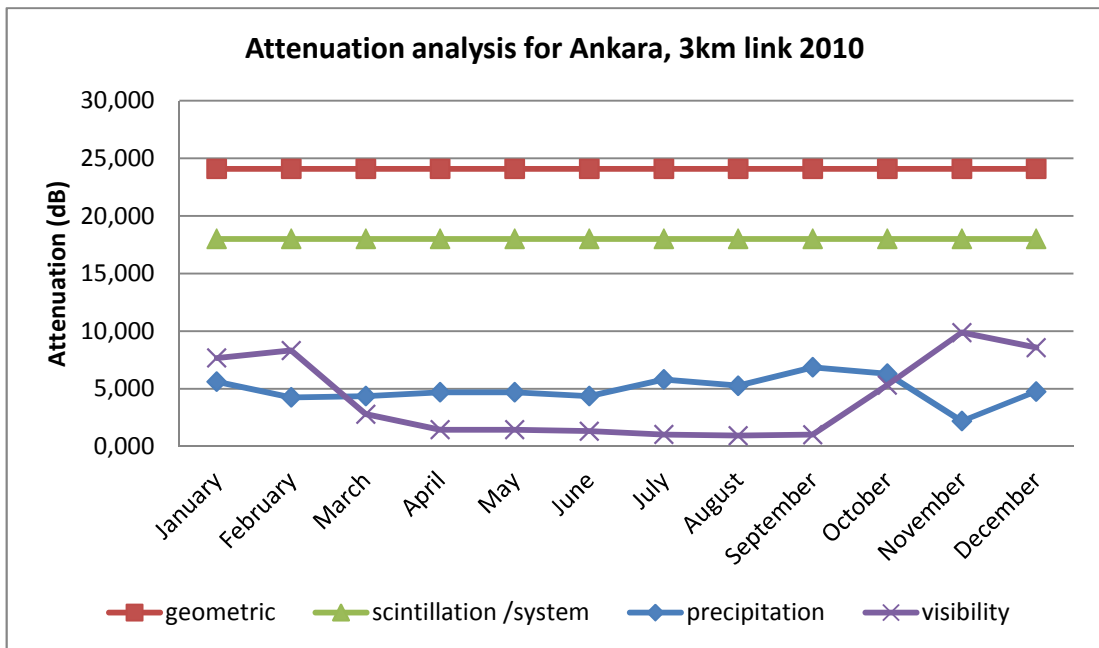Sessional effects on the attenuation and its participants can be observed in Fig.20-22 below.

Figure 20 Attenuation Analysis of 3 km Link for Ankara at Year 2010
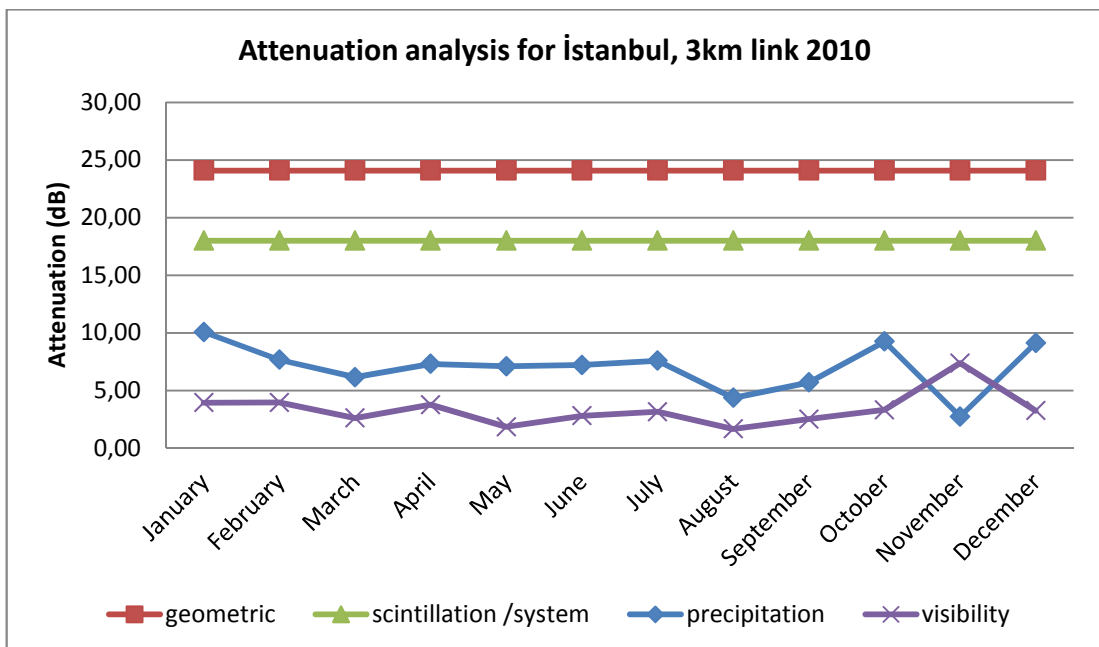
Figure 21 Attenuation Analysis of 3 km Link for İstanbul at Year 2010
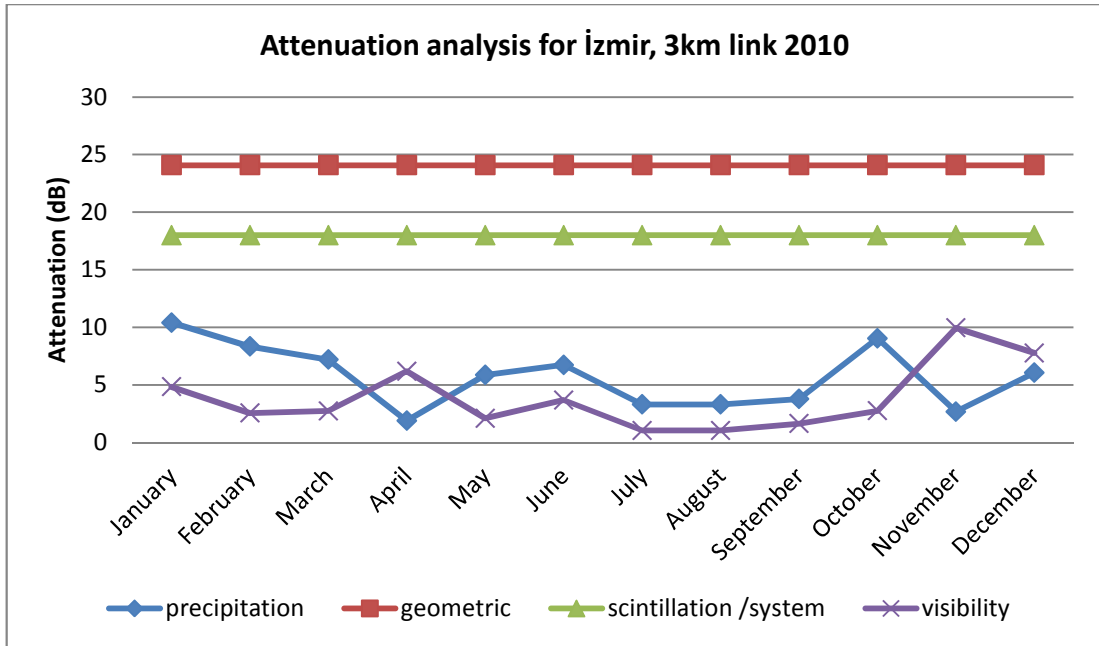
Figure 22 Attenuation Analysis of 3 km Link for İzmir at Year 2010

An attractive point is that in November, all three cities had seen almost 10 dB attenuation due to fog. One exception in İzmir the fog attenuation is higher than rain attenuation in April. Except that, fog is the major effect in Ankara while the rain in İzmir and İstanbul.

Another attractive point is that constant losses still dominate the total attenuation when the link distance is up to 3 kilometers. In theory, the effect of the constant losses should reduce when the link distance is increased. It can be seen in Fig.23 that the effect of the constant losses reduced with the range increment. However, it is still the major effect at three kilometers range.
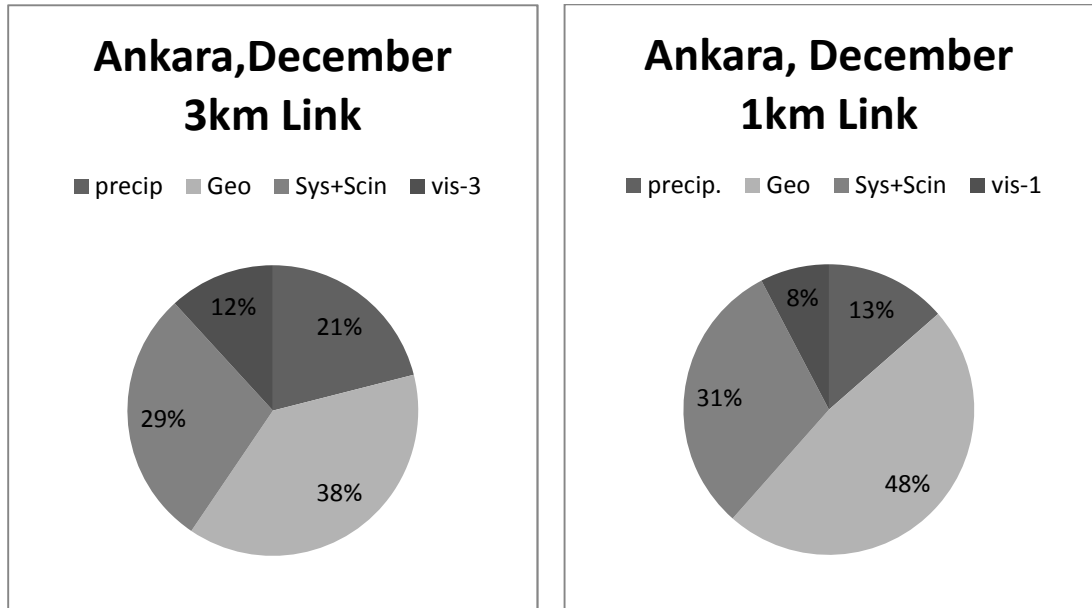
Figure 23 Distribution of Losses in Ankara in December for 1km and 3 km Links.

To see the daily behavior of FSO link, 10.12.2010 is selected as an example time interval and the daily changes on the visibility and on the availability values were plotted. As it seen in Fig.24, fog is generally seen in Ankara at late night and in early morning. Thus, unavailability for the link was observed at that time. When we have a look to foggy days in other days, same situation can be observed. Thus, it can be considered as a fact for Ankara.

In İstanbul, visibility has dramatically dropped in the morning. Effect of this drop on availability can be seen in Fig.25.

On the other hand, İzmir did not experience unavailability due to visibility on this day. Fig. 26 shows the visibility versus link availability graph for İzmir. In addition, this visibility behavior for all cities perfectly fits to meteorological statistics.

Figure 24 Visibility-Link Availability Graph on 10/12/2010 in Ankara
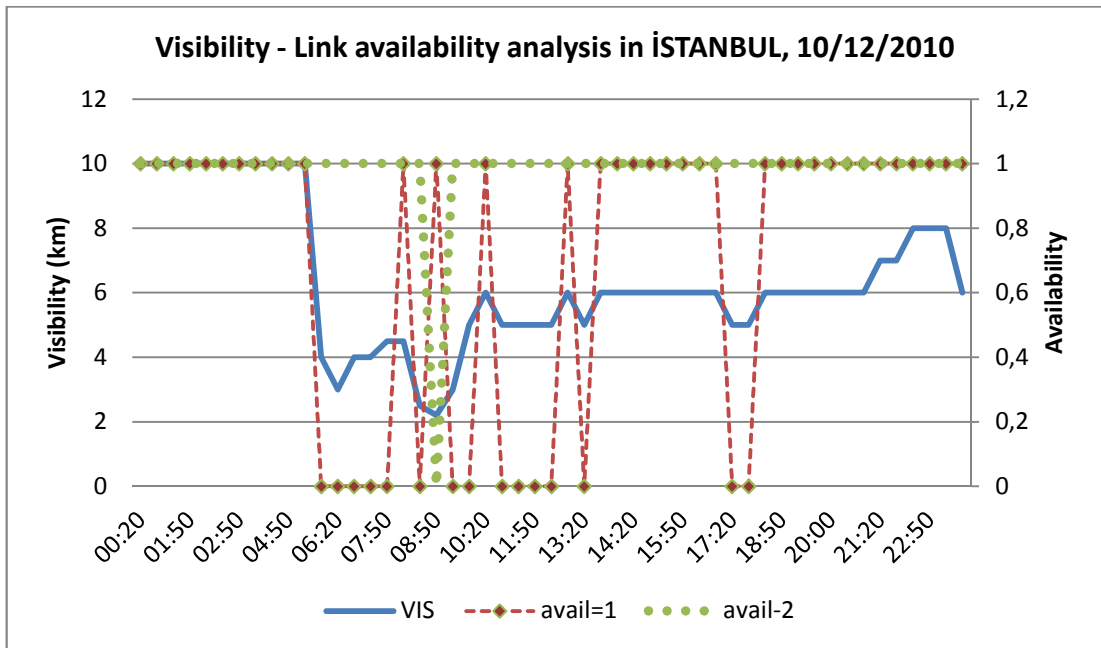
Figure 25 Visibility-Link Availability Graph on 10/12/2010 in İstanbul
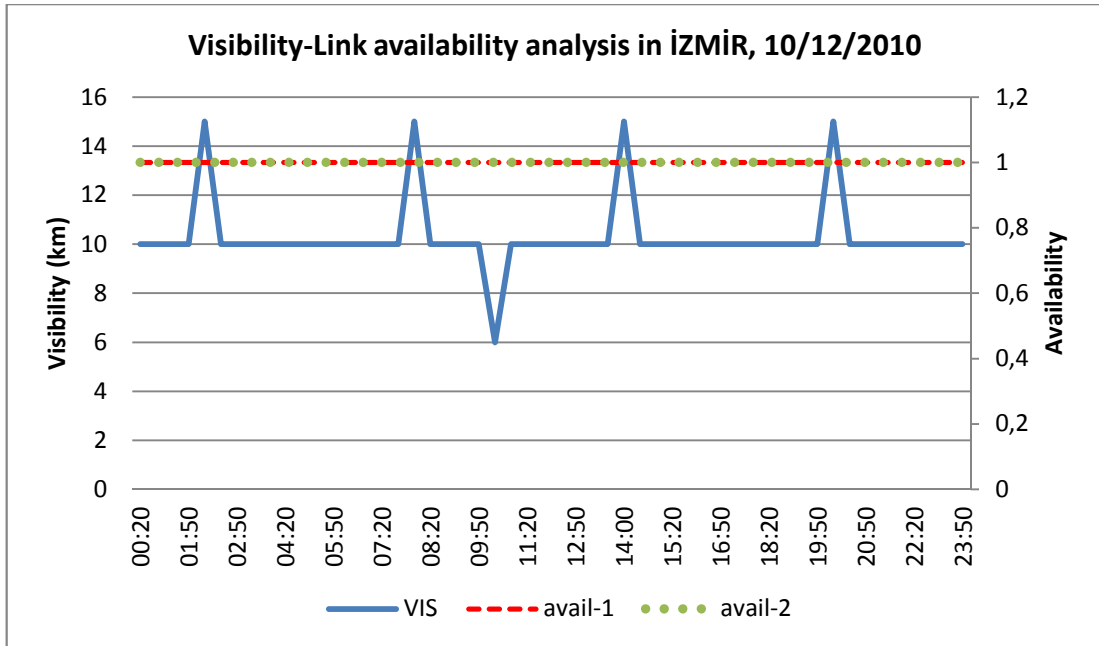
Figure 26 Visibility-Link Availability Graph on 10/12/2010 in İzmir
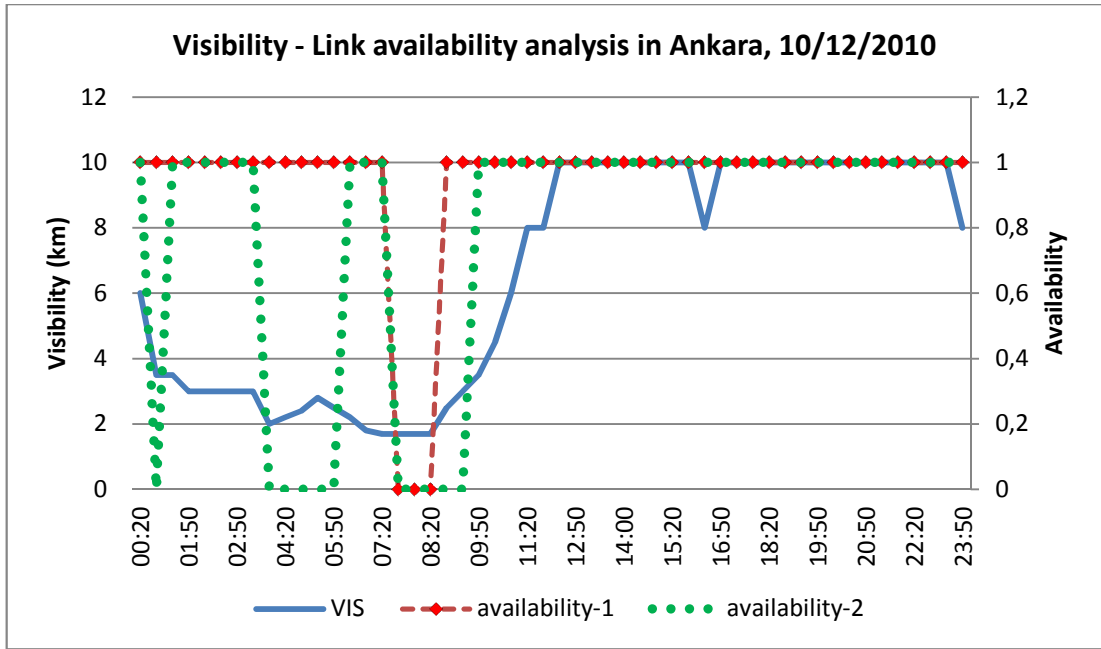
At last, overall link performances along the whole year were investigated. İzmir achieved the best availability values while Ankara was showing the worst performance as expected. Ankara experienced unavailability for all cases. As it can be seen in table 4, five months are fully and two months are almost fully available. Due to half an hour heavy rain, which causes 16,87dB attenuation, these two months were not fully available. In other months, attenuation generally caused by morning fog which can create over 70dB attenuation. In the most unfavorable month, along 68 hours the visibility was below one kilometer and the link was unavailable for one and a half hour even at case-1 with high power system.

In İstanbul, the availability values of case-1 and even case-2 with high power FSO system can provide communication channel with an acceptable quality. Like Ankara, availability values decrease in winter months due to generally precipitation but also the fog. table 5 gives the availability values of İstanbul.

Table 4 Annual Link Availability Analysis of Ankara (2010)

ANKARA								
Yearly	**Case**	**Link**	**January**	**February**	**March**	**April**	**May**	**June**
99,960%	Case -1	fso-1 1km	100,000%	99,731%	100,000%	100,000%	100,000%	100,000%
98,647%	Case-2	fso-1 3km	97,446%	98,253%	100,000%	100,000%	100,000%	100,000%
99,675%	Case-1	fso-2 1km	99,866%	99,530%	100,000%	100,000%	100,000%	100,000%
98,191%	Case-2	fso-2 3km	95,565%	97,581%	100,000%	99,933%	99,933%	100,000%
			July	**August**	**September**	**October**	**November**	**December**
	Case -1	fso-1 1km	100,000%	100,000%	100,000%	100,000%	100,000%	99,798%
	Case-2	fso-1 3km	100,000%	100,000%	100,000%	99,664%	97,849%	90,860%
	Case-1	fso-2 1km	100,000%	100,000%	100,000%	100,000%	99,798%	96,976%
	Case-2	fso-2 3km	100,000%	100,000%	100,000%	98,118%	97,782%	89,785%

Table 5 Annual Link Availability Analysis of İstanbul (2010)

İSTANBUL								
Yearly	**Case**	**Link**	**January**	**February**	**March**	**April**	**May**	**June**
100,000%	Case -1	fso-1 1km	100,000%	100,000%	100,000%	100,000%	100,000%	100,000%
99,509%	Case-2	fso-1 3km	98,454%	98,958%	100,000%	99,931%	100,000%	99,931%
100,000%	Case-1	fso-2 1km	100,000%	100,000%	100,000%	100,000%	100,000%	100,000%
97,780%	Case-2	fso-2 3km	93,347%	95,610%	99,530%	99,583%	99,933%	99,444%
			July	**August**	**September**	**October**	**November**	**December**
	Case -1	fso-1 1km	100,000%	100,000%	100,000%	100,000%	100,000%	100,000%
	Case-2	fso-1 3km	99,933%	100,000%	100,000%	99,530%	97,500%	99,798%
	Case-1	fso-2 1km	100,000%	100,000%	100,000%	100,000%	100,000%	100,000%
	Case-2	fso-2 3km	99,731%	100,000%	99,792%	94,086%	96,667%	95,565%

At last, as we mentioned repeatedly, İzmir showed the best performance in the result of this study. As it can be seen in table 6, for all the cases an availability value over 99 percent was obtained. With these results, İzmir seems to be the best candidate to operate FSO links beside Ankara and İstanbul.

Table 6 Annual Link Availability Analysis of İzmir (2010)

İZMİR								
Yearly	**Case**	**Link**	**January**	**February**	**March**	**April**	**May**	**June**
100,000%	Case -1	fso-1 1km	100,000%	100,000%	100,000%	100,000%	100,000%	100,000%
99,749%	Case-2	fso-1 3km	99,866%	100,000%	100,000%	100,000%	100,000%	100,000%
100,000%	Case-1	fso-2 1km	100,000%	100,000%	100,000%	100,000%	100,000%	100,000%
99,047%	Case-2	fso-2 3km	98,320%	96,577%	99,194%	99,722%	99,798%	99,722%
			July	**August**	**September**	**October**	**November**	**December**
	Case -1	fso-1 1km	100,000%	100,000%	100,000%	100,000%	100,000%	100,000%
	Case-2	fso-1 3km	100,000%	100,000%	100,000%	99,933%	98,542%	98,656%
	Case-1	fso-2 1km	100,000%	100,000%	100,000%	100,000%	100,000%	100,000%
	Case-2	fso-2 3km	100,000%	100,000%	100,000%	98,723%	98,125%	98,185%

Fig.27 and Fig.28 give the comparative link availability graphs of all cities for case-1. In addition, Fig.29 and Fig.30 give the availability graphs for case-2. Seasonal effects, link distance limitations and the most important regional changes can be easily observed on these graphs.
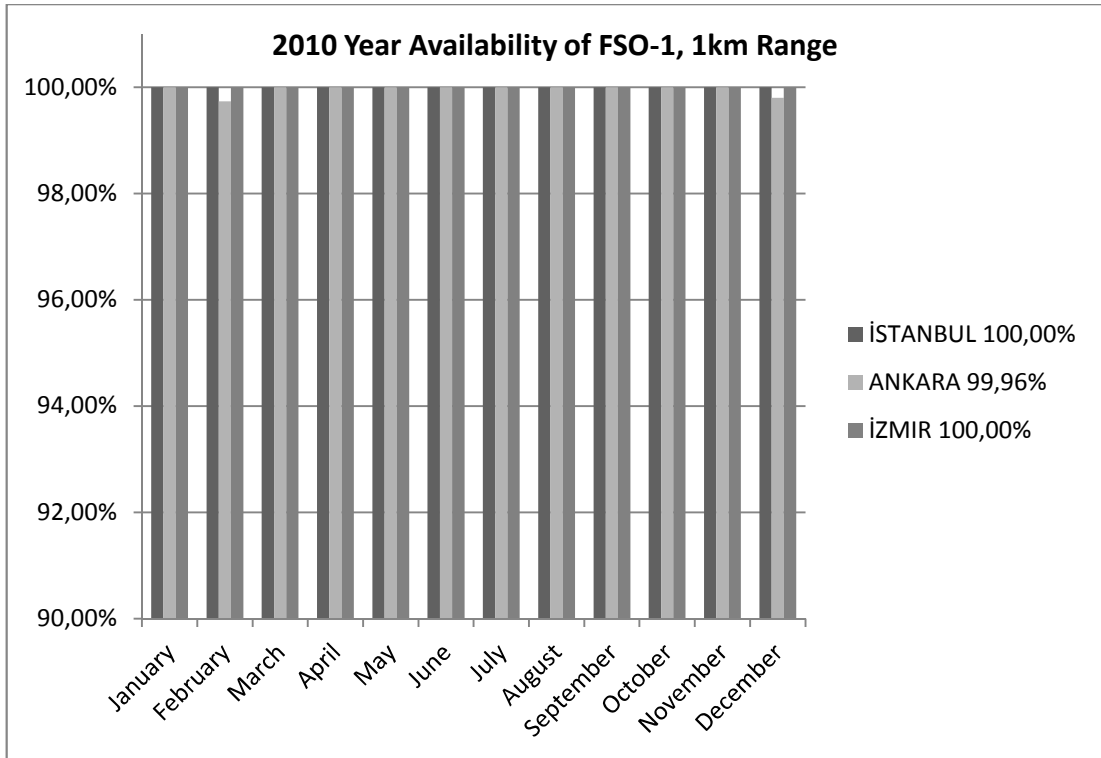
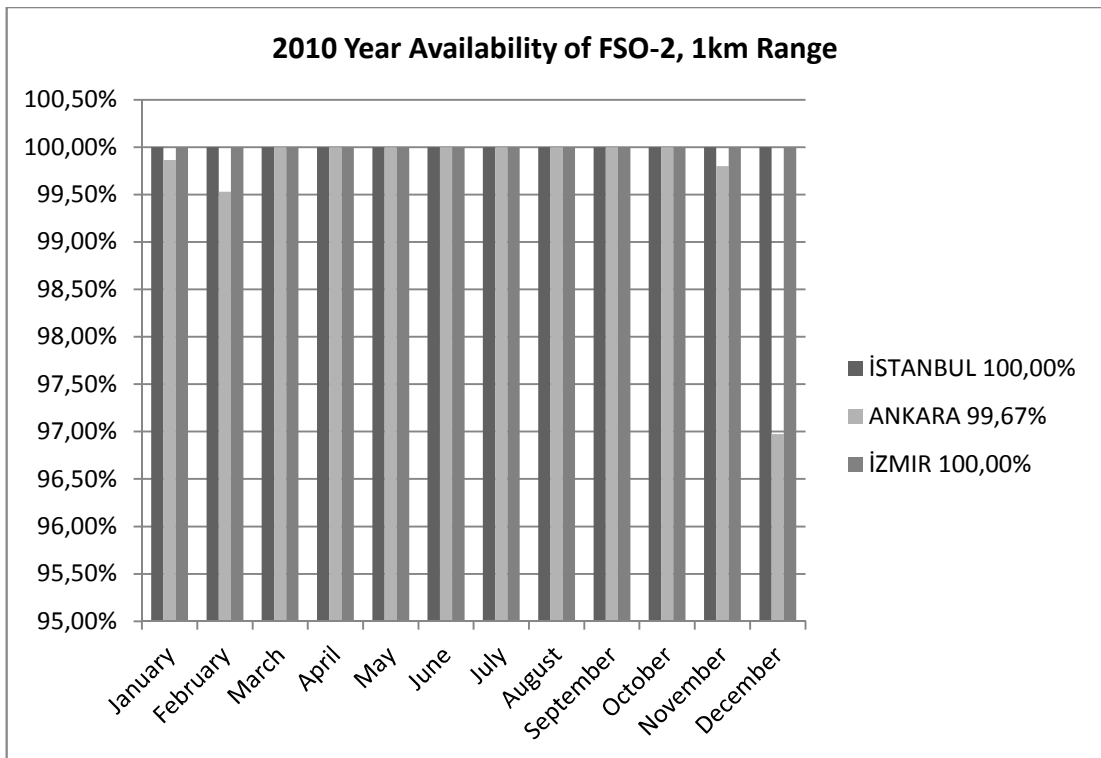**Figure 27** Comparative Link Availability Graphs of All Cities for Case-1, FSO-1

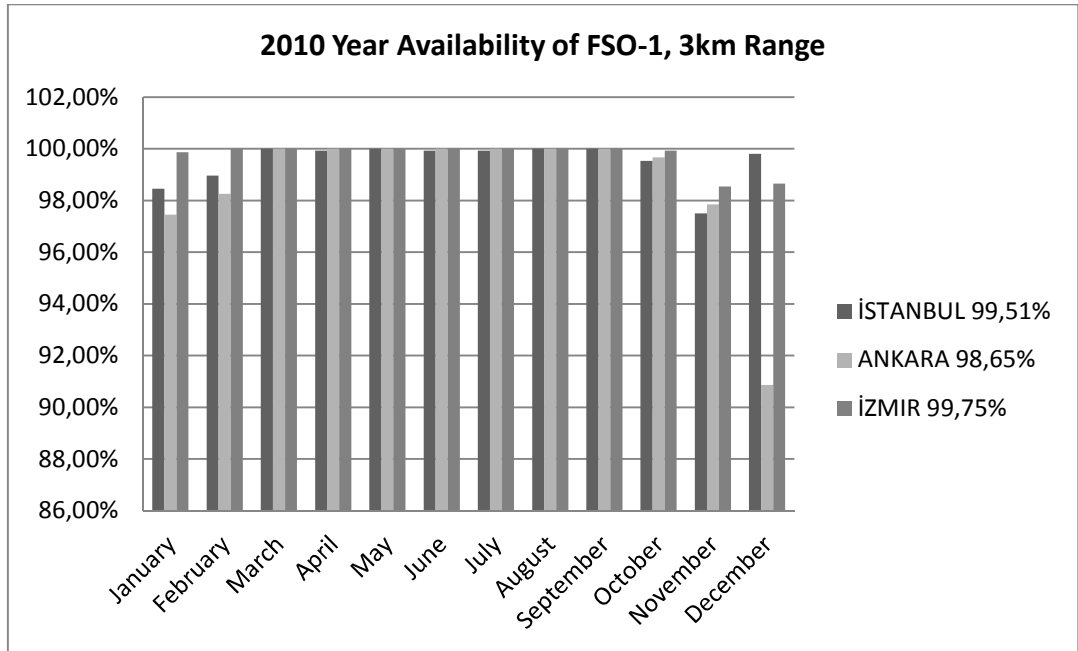**Figure 28** Comparative Link Availability Graphs of All Cities for Case-1, FSO-2

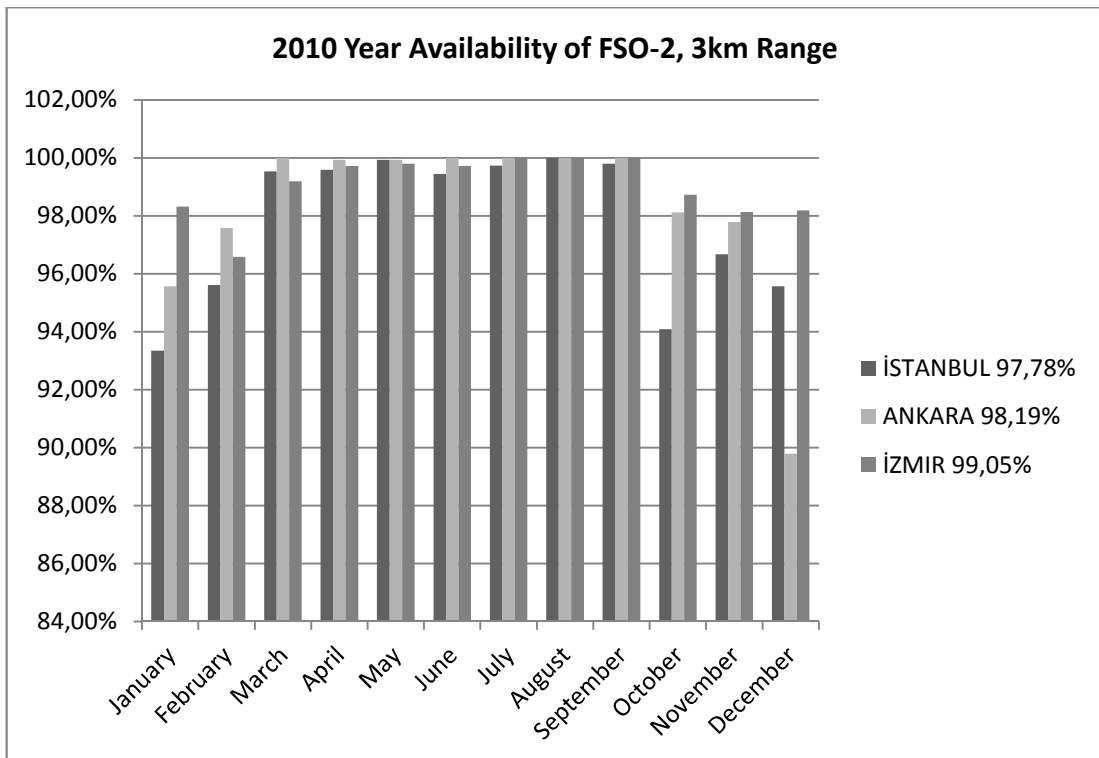**Figure 29** Comparative Link Availability Graphs of All cities for case-2, FSO-1

Figure 30 Comparative Link Availability Graphs of All cities for case-2, FSO-2

CHAPTER 6

CONCLUSION

Link availability is the key issue for free-space optical systems. This value can be increased by obtaining equipment reliability and network design with redundancy (for example with RF back up). However, the biggest unknown is the variable statistics of atmospheric attenuation. In this study we have tried to estimate the atmospheric attenuation by using statistical data gathered from airport stations around the Turkey. With the experimentally proven mathematical models and using MODTRAN code, to model the atmospheric attenuation, annular link availability values for Ankara, İzmir and İstanbul are presented.

For the short-range link (case-1), all cities showed a link availability performance over 99 percent, which is good enough for enterprise networks. However, FSO link in Ankara was not still fully available even with this range. According to link budget tables, which are given in Fig.16-18, the biggest factor of link unavailability in Ankara is the fog and it is accepted as the most severe effect of atmosphere on FSO links. The precipitation attenuation, which was commonly observed in İstanbul and İzmir, is not big enough to influence the total link availability at that range. In addition, constant losses like geometrical and system losses dominate the total attenuation at 1 km link.

For the long-range link (case-2), even precipitation was a problem. At that range, only İzmir achieved link availability over 99 percent. In İstanbul, only 97,78 percent

link availability could be provided with low power FSO system. This is the lowest availability value for the three cities. However, Ankara showed the worst performance again. It could not give a link availability value over 99 percent even with high power system.

This study gives a basic feasibility report for the users or companies about the deployable FSO links in Turkey. Using historical meteorological data, the severe effects were identified for the largest cities of Turkey.

However, out of some major airports in Turkey, the resolution of visibility measurements is generally 100 m or worse and the time interval is thirty minutes. Carrier-class links four 9s (99,99) or five 9s (99,999) cannot be predicted with these data set. A better data set is needed to more accurately predict the availability. To enable this, some special instruments, which can calculate the visibility and attenuation simultaneously, are needed. In addition, these instruments should make measurement more than one year to see the seasonal effects of weather conditions. Finally, a numerical model could be improved to analyze the effect of scintillation on the quality of the link. However, that requires collecting specific data from the atmosphere with own equipment to get reliable results.

In conclusion, a detailed link availability study was completed for given FSO systems at given ranges in Turkey. Although it is not detailed enough to write a carrier-class service level agreement, it will be a reference guide for the first steps of that brand new technology for Turkey.

REFERENCES

[1] **CARBONNEAU, T.H., WISELY, D.R.** (1997), *Opportunities and Challenges For Optical Wireless; The Competitive Advantage of Free Space Telecommunication Links in Today's Crowded Marketplace*, Wireless Technologies and Systems: Millimeter Wave and Optical, Proceedings of SPIE, 3232, 1997, 119-128.

[2] **AKBULUT, M. E. et. al.** (2003), *An Experimental Hybrid FSO/RF Communication System*, Proceeding (393) Communication Systems and Networks, 2003.

[3] **FREDRIK, SAKARI** (2002), *Design and Analysis of an All-Optical Free-Space Communication Link*, Levander, Per, Linköping University, Sweden.

[4] **MORADI, H., et. al.** (2010), *Availability Modeling of FSO Mesh Networks Through Turbulence-Induced Fading Channels*, IEEE INFOCOM 2010, San Diego, CA, March 2010.

[5] **FORIN, D. M., et. Al.** (2007), *Very High Bit Rates WDM Transmission on a Transparent FSO System*, ECOC 2007 - 33rd European Conference and Exhibition of Optical Communication, 2007.

[6] **CIARAMELLA, E., et. al.** (2009), *1.28-Tb/s (32 x40 Gb/s) Free-Space Optical WDM Transmission System*, IEEE Photonics Technology Letters - 21 : 1121 :1123 (2009)

[7] **XU, F., et. al** (2009), *Pulse Position Modulation for FSO Systems: Capacity and Channel Coding*, Ecole Centrale Marseille, Institut Fresnel, 2009

[8] **MUHAMMAD, S.S., LEITGAB, E.** (2005), *Multilevel Modulation and Channel Codes for Terrestrial FSO links*, Inst. of Broadband Comm., Tech. Univ. Graz, 2005.

[9] **WAINRIGHT, E., et. al.** (2005), *Wavelength Diversity in Free-space Optics to Alleviate Fog Effects*, Proc. SPIE 5712, 110.

[10] **KIM, I. et. al.** (2000), *Comparison of Laser Beam Propagation at 785 nm and 1550 nm in Fog and Haze for Optical Wireless Communications*, in Optical Wireless Communications III, vol. 4214 of Proceedings of SPIE, pp. 26–37, November 2000.

[11] **FERDINANDOV, E., et. al.** (2009), *A General Model of the Atmosphere Scattering in the Wavelength Interval 300–1100 nm*, Radioengineering, vol. 18, no. 4, pp. 517–521, 2009.

[12] **KRUSE, P., et. al.** (1962), *Elements of Infrared Technology*, John Wiley & Sons, New York, NY, USA, 1962.

[13] **MAHA ACHOUR, Ph.D.**(2003), *Free-Space Optics Wavelength Selection: 10 µ Versus Shorter Wavelengths*, Journal of Optical Networking, Vol. 2, Issue 6.

[14] ITU-R Report F.2106: Fixed Service Applications Using Free-Space Optical Link.

[15] **BOUCHET, O., et. al.** (2005), *FSO and Quality of Service Software Prediction*, in Proc. SPIE, Aug. 2005, pp. 28–39.

[16] **BOUCHET, O., et. al.**(2006), *Free Space Optics, Propagation and Communication*, ISTE, London, UK, 2006.

[17] **MICHELE D'AMICO, et. al.** (2003), *Free-Space Optics Communication Systems: First Results From a Pilot Field-Trial in the Surrounding Area of Milan*, Italy IEEE MICROWAVE AND WIRELESS COMPONENTS LETTERS, VOL. 13, NO. 8, AUGUST 2003.

[18] **ZDENEK KOLKA, et. al.** (2010), *Availability Study of FSO Systems in Europe*, World Scientific and Engineering Academy and Society (WSEAS) Stevens Point, Wisconsin, USA 2010.

[19] **KIM, I., KOREVAAR, E.** (2001), *Availability of Free Space Optics (FSO) and Hybrid FSO/RF Systems*, Proc. SPIE Optical Wireless Communication IV, vol. 530, pp. 84-95, Denver CO, 21-22 August 2001.

[20] **AKBULUT, A., et. al.** (2005), *Design, Availability and Reliability Analysis on an Experimental Outdoor FSO/RF Communication System*, IEEE ICTON, pp.403-406, 2005.

[21] Merrill Lynch Global Securities and Economics Group (2001), *Free Space Optics*, 15 May 2001.

[22] **STEEGE, M.** (2001), *Free-Space Optics: A Viable, Secure Last-Mile Solution*, GSEC, 2001. Retrieved at: http://freespaceoptic.com/WhitePapers/FSOSecurity.doc (Last retrieved on 10 July 2011).

[23] **KIM, I, et. al.** (1998), *Wireless Optical Transmission of Fast Ethernet, FDDI, ATM, and ESCON Protocol Data Using the TerraLink Laser Communication System*, Optical Engineering, Vol. 37 No. 12, December 1998.

[24] **HEINZ, A., et. al.** *Fiber Optics Without Fiber*, Retrieved at: http://www.freespaceoptic.com/Fiber_Optics_Without_Fiber.htm (Last retrieved on 10 July 2011).

[25] **TOLKER-NIELSEN, T., GUILLEN, J.C.** (1998), *SILEX: The First European Optical Communication Terminal in Orbit*, ESA Bulletin Nov 1998.

[26] **STREET, A. M., et. al.** (1997), *A Review on Indoor Optical Wireless Systems, Optical and Quantum Electronics*, 29(3), 349-378. Springer.

[27] Retrieved at: http://en.wikipedia.org/wiki/Infrared_Data_Association (Last retrieved on 10 July 2011).

[28] **OGAWA, H.** (2009), *Recent Progress and Standardization of Terrestrial Wireless and Satellite Communication Systems*, in NTC Int. Conf., Mar. 2009.

[29] **BLOOM., S., et. al.** (2003) *Understanding the Performance of Free- Space Optics, Journal of Optical Networking*, pp. 178-200, June 2003.

[30] **BARCLAY, L. W.** (2002), *Terahertz Propagation,* Lancaster University, Book: Propagation of Radiowaves, Published Dec 2002.

[31] **DAVID A. JOHNSON** (2006), *Optical Through the Air Communications Handbook*, Retrieved at: http://www.imagineeringezine.com/files/air-bk2.html (Last retrieved on 10 July 2011).

[32] **AL NABOULSI, M., et. al.** (2005), *Propagation of Optical and Infrared Waves in the Atmosphere*; 28th AG URSI ; New Delhi (India) ; 23-29 October 2005.

[33] **ANDREWS, L.C., et. al.** (2001), *Laser Beam Scintillation with Applications*, Bellingham: SPIE Press, 2001.

[34] **WILLEBRENT, H., GHUMAN, B.S.** (2002), *Free-Space Optics: Enabling Optical Connectivity in Today's Networks*, Indianapolis: Sam's Publishing, 2002.

[35] Rec. ITU-R P.1814 (2007), *Prediction Methods Required for the Design of Terrestrial Free-Space Optical Links*.

[36] **NADEEM, F., et. al.** (2008), *Comparing the Fog Effects on Hybrid Network Using Optical Wireless and GHz Links,* International Symposium on Communication Systems, Networks and Digital Signal Processing, pp. 278-282, July 2008.

[37] Glossary of Meteorology (June 2000). *Rain*. American Meteorological Society, Retrieved on 2011-06-15.

[38] **ANDREWS, L. C.** (2004), *Field Guide to Atmospheric Optics*, Washington: SPIE Press, 2004.

[39] **ANDREWS, L. C., PHILLIPS, R. L.** (1998), *Laser Beam Propagation through Random Media*, SPIE – The International Society for Optical Engineering, 1998.

[40] **DORDOVA, L., WILFERT, O.** (2010), *Calculation and Comparison of Turbulence Attenuation by Different Methods*, Radioengineering. 2010. 19(1). p. 162 – 167.

[41] **BENDERSKY, S. et. al.** (2004), *Atmospheric Optical Turbulence Over Land in Middle East Coastal Environments: Prediction Modeling and Measurements*, Appl. Opt. 43, 4070-4079 (2004).

[42] **BEN-YOSEF, N., et. al.** (1979), *Refractive-index Structure Constant Dependence on Height*, J. Opt. Soc. Am., vol. 69,pp. 1616–1618, 1979.

[43] **TATARSKII, V. I.** (1971), *The Effects of the Turbulent Atmosphere on Wave Propagation*, Translations for NOAA by the Israel Program for Scientific Translations, Jerusalem, 1971.

[44]   Weather Underground Company, http://english.wunderground.com/history/ (retrieved several times in 2011)

[45] **BLOOM, S., HARTLEY, W.** (2002), *The Last-Mile Solution: Hybrid FSO Radio*, in Whitepaper, AirFiber Inc., May 2002.

[46] **NYKOLAK, G., et. al.** (2000), *A 160 Gb/s Free Space Transmission Link*, in Proceedings of 2000 CLEO, Paper PD15, (IEEE, Washington, D.C., 2000).